Sustainable Marine Structures
https://journals.nasspublishing.com/index.php/sms

ARTICLE

Multi-Criteria Site Suitability Assessment for Nearshore Floating Solar Photovoltaic Systems in the Gulf of Thailand: Integrating Hydrodynamic, Economic, and Environmental Factors

Kornpaphop Ruttanawijit [1], ***Taweesup Desua*** [1], ***Yodchai Tiaple*** [2*]

[1] *Department of Energy Technology, Faculty of Engineering and Industry Technology, Rambhai Barni Rajabhat University, Chanthaburi 22000, Thailand*

[2] *Department of Maritime Engineering, Faculty of International Maritime Studies, Kasetsart University, Sriracha Campus, Chonburi 20230, Thailand*

ABSTRACT

The paper provides a macro-level screening procedure for nearshore floating photovoltaic (N-FPV) suitability using province-level analysis based on Analytic Hierarchy Process (AHP)-Technique for Order Preference by Similarity to Ideal Solution (TOPSIS) multi-criteria decision making supported by entropy objective weighting validation. The study assesses nine coastal provinces based on the following factors: irradiance, wave height, wind velocity, tidal range, coastal erosion, current velocity, proximity to existing grids, and industrial demand utilizing ERA5 reanalysis data (2019–2023) validated by 31 in-situ stations in the region. The inter-factor independence is confirmed with Pearson correlation analysis ($|r| < 0.70$ for all pairings), and asymmetric wind factor penalties are introduced to improve the physical realism of the ranking. Rayong ($Ci = 0.741$) and Chonburi ($Ci = 0.682$) are selected as tier 1 regions because of their high irradiance levels (5.15–5.29 kWh/m^2/day), moderate waves ($Hs = 0.48$–0.52 m), and high-quality industrial infrastructure along the Eastern Economic Corridor. The results are further validated with ViseKriterijumska Optimizacija I Kompromisno Resenje (VIKOR) cross-checking, entropy weighting, demand proxy analysis, and criteria structure modification. The proposed

*CORRESPONDING AUTHOR:
Yodchai Tiaple, Department of Maritime Engineering, Faculty of International Maritime Studies, Kasetsart University, Sriracha Campus, Chonburi 20230, Thailand; Email: yodchai.ti@ku.th

ARTICLE INFO
Received: 20 March 2026 | Revised: 6 April 2026 | Accepted: 15 April 2026 | Published: 7 May 2026
DOI: https://doi.org/10.36956/sms.v8i2.3210

CITATION
Ruttanawijit, K., Desua, T., Tiaple, Y., 2026. Multi-Criteria Site Suitability Assessment for Nearshore Floating Solar Photovoltaic Systems in the Gulf of Thailand: Integrating Hydrodynamic, Economic, and Environmental Factors. Sustainable Marine Structures. 8(2): 82–112.
DOI: https://doi.org/10.36956/sms.v8i2.3210

approach shows strong stability to weight perturbations of up to ±22%. A techno-economic analysis of a 10 MWp system results in a range of Levelized Cost of Electricity (LCOE) values between \$0.096–\$0.111/kWh (Monte Carlo 50th percentile (P50): \$0.097–\$0.112/kWh). The scale analysis reveals a 12–18% reduction in costs per kilowatt of output at 5–50 MWp capacity levels. Project feasibility relies heavily on corporate power purchase agreements at or above \$0.12/kWh; currently, the feed-in tariff is at \$0.08/kWh, which leads to negative returns. Carbon credits can provide additional income. The results can be interpreted as provincial tiers before the actual screening of site locations; Geographic Information System (GIS) exclusion mapping and extreme-event studies should be considered mandatory.

Keywords: AHP-TOPSIS; Province-Level Pre-Screening; Eastern Economic Corridor; Levelized Cost of Electricity; Corporate Power Purchase Agreement; Marine Renewable Energy

1. Introduction

1.1. Background and Rationale

Given the increasing global emphasis on the shift towards low-carbon energy, much attention has been paid to solar photovoltaic (PV) technologies as scalable and economically feasible alternatives among renewable energy sources. By 2023, global solar PV power capacity had reached 1,500 GW, adding over 400 GW annually; hence, solar energy has become the most rapidly growing source of electricity [1]. Nonetheless, spatial limitations increasingly restrict the growth potential of ground-mounted solar PV installations within densely populated areas, including coastal Asia, due to the competing use of the same land for agriculture, urban development, and conservation purposes [2]. Such limitations have led to the development of floating photovoltaic (FPV)—systems that utilize solar panels mounted on water surfaces, keeping land available for alternative uses. FPVs have evolved from early applications in freshwaters to being installed in more difficult marine conditions. FPVs have been shown to provide additional benefits to those already provided by standard PVs; these include the reduction in evaporative loss, increased panel efficiency owing to efficient water cooling, and the suppression of algal bloom development due to surface shading [3]. By 2023, the total FPV capacity has been estimated to be 6 GW and is projected to grow up to 60–70 GW in 2030 due to the decreasing cost of FPV technology and the exhaustion of reservoir locations [4]. Consequently, the development of nearshore floating photovoltaics (N-FPVs) has emerged as the next step forward in the FPV sector, as nearshores represent far greater spatial resources compared to reservoirs. Being intermediate between protected inland installations and challenging offshore facilities, N-FPVs are usually located between 2–10 km off the shoreline and in depths of 5–30 m; thus, these locations are characterized by lower exposure to wave energy as compared to offshore but without extreme engineering challenges typical for deep-water offshore PVs [5]. Given high solar irradiation (annual averages: 4.5–5.5 kWh/m^2/day), long coastlines, high electricity consumption rates, and a strong commitment to renewables in Southeast Asia, N-FPVs can be considered highly applicable in Southeast Asia. According to the official goals, Thailand plans to operate carbon-neutrally by 2050 and will have to significantly increase its power generation using renewables, with a floating solar capacity target set at 2.7 GW [6]. As the part of the Thai territory, the Gulf of Thailand can be considered partially closed off-shore waters, having around 2,500 km of the coastline and average wave height ranging from 0.5 to 1.2 m [7–9]. Nonetheless, despite these opportunities for N-FPV deployment, there seems to be little research focused on systematic province-level screening for N-FPVs in the Gulf of Thailand area. While the development strategy of Thailand (PDP2024) explicitly aims at further growth of floating solar energy, no screening mechanisms exist that would consider the peculiarities of nearshore installation, such as seasonal wave exposure, tidal current loads, and competition of uses in the marine area. Therefore, the selection of the promising provinces without the use of a proper screening method will lead to subsequent issues regarding permit acquisitions and financing. Multi-Criteria Decision Analysis (MCDA)-Techno-Economic Analysis or Assessment (TEA) framework will be of great use in such circumstances.

Recent advances in offshore and nearshore FPV have provided increasingly relevant technical and economic evidence. Comprehensive reviews of FPV reliability in harsh marine environments [10] and marine environmental protection considerations for offshore FPV plants [11] have highlighted the critical importance of wave-resistant structural design, mooring fatigue, and ecological impact mitigation for sea-based deployments. Global techno-economic assessments of offshore FPV potential have demonstrated that Southeast Asian locations—including Thailand and Malaysia—could achieve LCOE values below \$0.06/kWh under favorable conditions [12], while Mediterranean LCOE mapping has revealed that installation costs increasing with distance to shore constitute the dominant cost driver [13]. Site selection methodologies using GIS-FAHP (Fuzzy Analytic Hierarchy Process) and GIS-AHP-MCDA approaches have been successfully applied to FPV in Turkey [14], Bangladesh [15], and coastal India [16], demonstrating the broad applicability of multi-criteria frameworks to diverse geographic contexts. Mooring system design for shallow-water FPV arrays has received increasing attention, with comparative analyses of catenary and taut mooring configurations [17] and hydrodynamic studies of nearshore FPV under seabed topography effects [18] providing essential engineering guidance for nearshore deployments. Techno-economic feasibility studies of FPV on offshore oil platforms [19] and life cycle cost analyses for North Sea FPV concepts [20,21] have further expanded the economic evidence base. These studies collectively inform the present work by establishing both the technical feasibility envelope and the economic benchmarks against which Gulf of Thailand N-FPV screening results can be contextualized.

1.2. Literature Review

In Scopus and Web of Science, a comprehensive search was conducted with the following strings: ("floating photovoltaic" OR "FPV") AND ("site suitability" OR "MCDA" OR "AHP") AND ("marine" OR "nearshore" OR "coastal"). In total, 312 records were found, out of which 47 papers passed the title and abstract screening for relevance to marine or nearshore FPV. A supplementary search using "floating photovoltaic", "Gulf of Thailand", and "site suitability" confirmed that no prior systematic province-level assessment has been done, implying the novelty of the current study. The nearshore marine environment presents different challenges such as corrosion due to saltwater, biofouling, wave motion effects on platforms, and mooring difficulties that distinguish it from freshwater floating photovoltaics (FPVs) [22,23]. Successful pilot projects in Singapore, South Korea, and the Netherlands prove that the technology is feasible, with a 5 MW installation in Woodlands providing valuable field data for tropical nearshore applications [24]. It is evident that N-FPV systems can perform competitively as long as the environmental and site-related characteristics are harmonized with system design parameters. Multi-criteria decision analysis (MCDA) offers a structured procedure for assessing the appropriateness of a choice among different alternatives, especially those with conflicting goals [25]. The Analytic Hierarchy Process (AHP), proposed by Saaty in 1980 [26], is an excellent methodology for eliciting experts' opinions for determining the weights of criteria. The Technique for Order Preference by Similarity to Ideal Solution (TOPSIS) offers a sound mathematical basis for ranking alternatives based on their proximity to ideal performance for each criterion [25]. Together, the AHP-TOPSIS combination has been widely applied in the context of renewable energy site selection for onshore wind, ground-mounted solar, and offshore wind energy infrastructure [27–30]. Most MCDA-based FPV site suitability studies use criteria related to inland water bodies (e.g., reservoir depth, water quality, evaporation effects) or criteria for offshore wind farms in marine environments [25]. None of the criteria are relevant for tropical monsoon regions because N-FPVs operate in a completely different regime. Furthermore, most prior research ends at the suitability ranking stage without considering whether the best-ranked sites would be economically viable with local tariffs.

One of the critical limitations associated with the use of subjective AHP weighting methods, especially for small groups of experts, is the potential for the ranking process to be significantly influenced by limited stakeholder bias. Current research within the field of MCDA suggests that it would be beneficial to include at least one of the following objective weighting methods as part of AHP (entropy, Criteria Importance Through Intercriteria Correlation or CRITIC), in order to determine if the ranks generated depend on the methodology used or if they accurately represent true patterns in the dataset [29,31]. This paper uses entropy weighting as an objective weighting technique (Section 3.3.1). Previous studies on floating photovoltaics in Thailand have almost exclusively been concerned with inland reservoirs, especially hydropower plants for which power connection infrastructure and reservoir surface area are guaranteed [32]. Studies concerning offshore floating solar farms have tended to focus on Atlantic regions of Europe and the North Seas, along with East Asia, with minimal work performed in monsoonal semi-closed seas [33,34]. In addition, the utilization of integrated MCDA techniques for FPV near-shore deployment has been largely overlooked thus far, as previous work has tended to focus on inland FPV reservoir selection [29,32,35].

1.3. Research Objectives

This study addresses the identified knowledge gap by developing a province-level pre-screening framework for N-FPV deployment in the Gulf of Thailand. The research integrates AHP-derived criteria weights with TOPSIS-based provincial ranking to evaluate nine coastal provinces distributed around the Gulf perimeter, encompassing the eastern seaboard industrial corridor, inner Gulf zones, and southern coastal areas. The assessment framework incorporates eight evaluation criteria spanning solar resource potential, oceanographic conditions, coastal vulnerability, and techno-economic factors, with criteria weights elicited from a panel of domain experts and cross-validated against entropy-based objective weighting.

The study pursues four specific objectives: (1) to establish a multi-criteria evaluation framework incorporating technical, environmental, and economic dimensions relevant to nearshore marine solar pre-screening; (2) to quantify provincial-level performance across Gulf of Thailand coastal provinces using the Fifth generation of the ECMWF atmospheric reanalysis (ERA5) reanalysis data validated against in-situ observations, with explicit acknowledgment of spatial resolution limitations; (3) to derive priority rankings identifying provinces with highest N-FPV macro-screening potential, validated through multiple robustness tests including VIKOR cross-validation, entropy weighting comparison, and an altered criteria structure experiment; and (4) to assess indicative techno-economic feasibility including levelized cost of electricity (LCOE) with Monte Carlo uncertainty propagation, scale sensitivity analysis, and financial return metrics under alternative revenue scenarios. These objectives collectively address the research question:

> *Which coastal provinces in the Gulf of Thailand present the most favorable conditions for near-shore floating photovoltaic macro-screening, and what indicative techno-economic performance can be anticipated at priority sites under acknowledged uncertainty?*

The research contributes to the emerging N-FPV literature in several dimensions. Methodologically, the study demonstrates the application of AHP-TOPSIS hybrid MCDA to marine floating solar pre-screening, supplemented by entropy-based objective weighting and correlation analysis to address criteria independence and weighting subjectivity. Empirically, the analysis generates the first systematic characterization of N-FPV pre-screening suitability across Thai coastal provinces—confirmed by exhaustive Scopus and Web of Science searches that returned no prior provincial-scale MCDA study for this region. To prevent ambiguity, the study outputs are explicitly defined as: (i) provincial priority tiers for N-FPV macro-screening (not site-specific deployment maps); (ii) an uncertainty-aware ranking sensitivity envelope; and (iii) indicative financial thresholds (tariff and Capital Expenditure (CAPEX) break-even) for commercialization. These outputs are designed to guide policy makers (macro-allocation) and developers (project pipeline screening), with mandatory GIS-based exclusion mapping and site-specific extreme-event analysis required before any deployment decision.

2. Study Area

2.1. Geographic Scope and Provincial Selection

The Gulf of Thailand is a semi-enclosed sea body within the South China Sea surrounded by Thailand, Cambodia, Vietnam, and Malaysia. The coastline of Thailand spans about 2,500 km within the Gulf region, featuring varied coastal environments from deltaic mudflats on the inner side of the Gulf to rocky cliffs and sand beaches on its eastern and western coasts [36]. Such variation in geography leads to variable environments for offshore floating PV power plant development, thus requiring a thorough analysis at the provincial level in the Gulf of Thailand region. **Figure 1** shows the study area, highlighting the nine selected coastal provinces in the Gulf of Thailand and the Eastern Economic Corridor border.

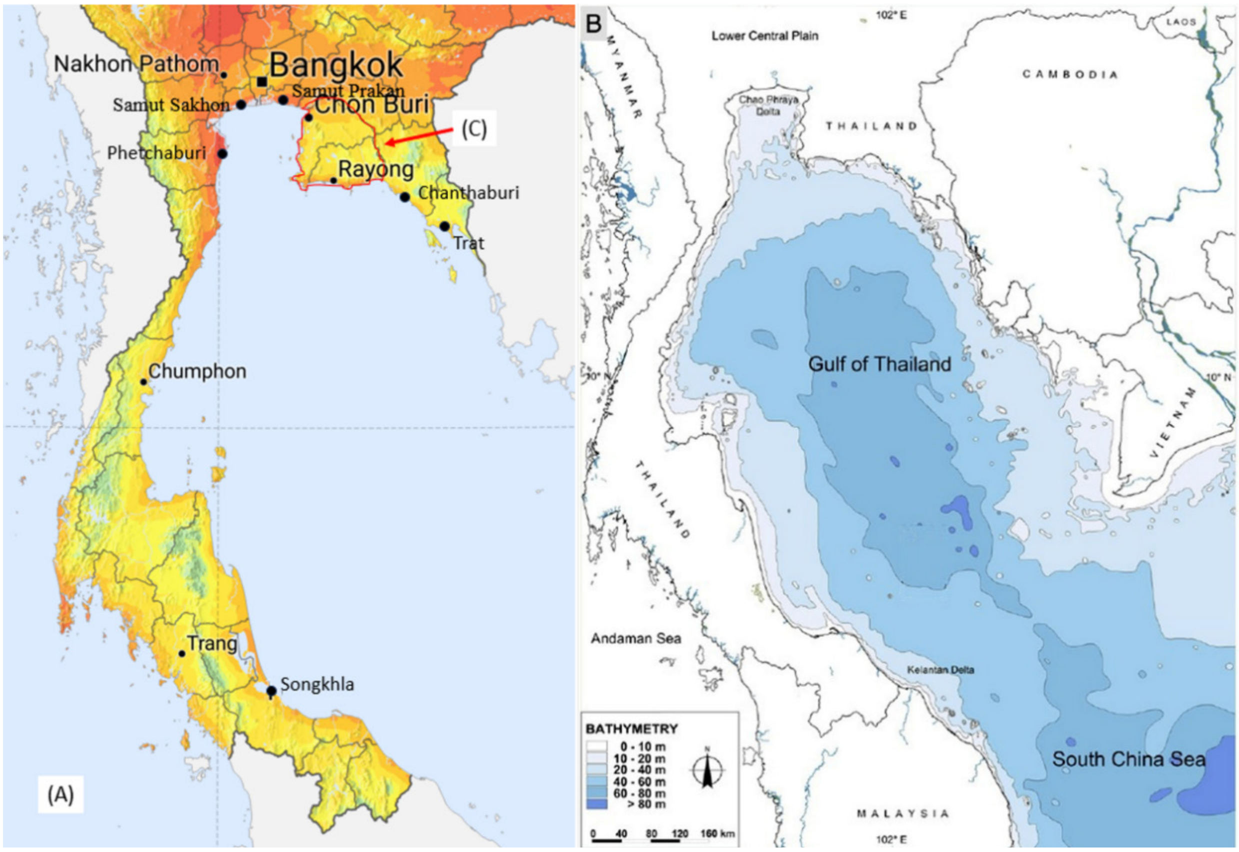

Figure 1. Study area map showing the Gulf of Thailand with nine evaluated coastal provinces (**A**), bathymetric contours (**B**), and the Eastern Economic Corridor (EEC) boundary (**C**).

The current research involves evaluating nine provinces located along the Gulf of Thailand to represent the most prevalent types of coasts and the corresponding development environment for preliminary N-FPV screening. The selected provinces include: (1) coasts exposed directly to the Gulf of Thailand; (2) coasts within 50 km proximity to the power grid; (3) coasts without the designation of marine protection areas that prevent energy development; and (4) geographically distinctive provinces covering the inner Gulf, eastern coast, western Gulf, and southern coast. Another practical criterion pertains to the depth and suitability of the nearshore bathymetric characteristics for mooring. According to the limitations on the feasibility of nearshore FPV engineering technology, provinces up to 10 km away from the coast and having depths ranging from 5 to 30 m are considered suitable for energy development, while areas farther than 10 km and at greater depths are excluded from further assessment.

Provinces are ranked based on provincial aggregates of the nearshore median suitability scores. A particular province can contain highly suitable as well as unsuitable areas (e.g., sheltered bays vs. exposed headlands or port-related areas vs. open coastlines); however, this information is reduced to a single metric for macro-screening purposes. Intra-provincial spatial variability is indicated by the inter-quartile range (IQR) reported in decision matrix for N-FPV provincial pre-screening; however, this does not eliminate the need for further GIS analysis to determine deployable polygons in top-ranking provinces. In total, nine provinces represent over 1,060 km of coastline across all environmental settings within the nearshore Gulf of Thailand region. The eastern seaboard provinces (Chonburi, Rayong, Chanthaburi, Trat) are part of Thailand's major industrial zone in the Eastern Economic Corridor (EEC), which possesses high electricity demand and existing grid connections, although there is moderate exposure to waves [37]. The inner Gulf provinces (Samut Prakan, Samut Sakhon) have sheltered locations without wave energy but may pose problems in terms of sediment transport and water quality. The western Gulf provinces (Phetchaburi, Chumphon) have moderate exposures with seasonal influence from monsoons, whereas the southern province (Songkhla) is located in the lower Gulf region with unique oceanography. **Table 1** provides details about each province.

Table 1. Nine coastal provinces selected for N-FPV macro-screening assessment.

No.	Province	Region	Coastline (km)	Coordinates	Key Characteristics
1	Samut Prakan	Inner Gulf	47	13.55° N, 100.52° E	Chao Phraya estuary, industrial zone
2	Samut Sakhon	Inner Gulf	41	13.45° N, 100.28° E	Mudflat coast, aquaculture
3	Chonburi	Eastern Seaboard	156	13.15° N, 100.98° E	EEC industrial hub, deep port
4	Rayong	Eastern Seaboard	105	12.65° N, 101.45° E	Map Ta Phut industrial estate
5	Chanthaburi	Eastern Seaboard	78	12.35° N, 102.15° E	Mixed rocky-sandy coast
6	Trat	Eastern Seaboard	165	11.95° N, 102.55° E	Island archipelago, sheltered bays
7	Phetchaburi	Western Gulf	92	12.45° N, 99.95° E	Mangrove-fringed coast
8	Chumphon	Western Gulf	222	9.95° N, 99.45° E	Transitional zone, moderate exposure
9	Songkhla	Southern Gulf	158	7.15° N, 100.60° E	Lagoon system, fishing port

2.2. Oceanographic and Climate Conditions

The Gulf of Thailand has certain distinct features of oceanography that make it different from other open sea areas and influence the design of N-FPVs accordingly. The fact that it is semi-closed and its deepest area reaches a depth of only 85 m, while its average depth equals roughly 45 m, makes it less stormy compared to the nearby South China Sea [8]. Average significant wave heights vary from 0.3–0.5 m for the inner part of the Gulf and from 0.5–0.9 m for the eastern coast, with a possibility of waves up to 2.0–2.5 m high during monsoon periods [9] in **Table 2**. Extreme event caveat: While extreme meteo-oceanic conditions have not been directly modeled in this provincial pre-screening exercise, it is known that the Gulf of Thailand is episodically affected by tropical depressions and abnormal monsoon surges capable of producing wave heights of 2.0–3.5 m and onshore gusts greater than 25 m/s. It is the extreme conditions, and not the mean state conditions used in the TOPSIS analysis, that determine the viability of structural survival, mooring requirements, and insurance considerations for any N-FPV installation [5,38]. While a province rated as suitable according to its mean state Hs may prove unsuitable due to poor design storm conditions, this ranking is merely indicative of suitable average operating conditions, not a guarantee of structural viability. Extreme value analyses on a site-by-site basis (e.g., significant wave height, wind gust, and storm surge for a 50-year return period) are required before deployment in any Tier 1 province as part of the Front-End Engineering Design (FEED) process.

Monsoonal effects on the Gulf result in pronounced seasonality, which determines the nature of both the wave climate and available solar resources. Northeast monsoons occur between November and February, with prevailing winds blowing from the northeast and leading to southwestward-moving wave fields. During the northeast monsoon period, the east coast provinces experience less energetic waves (mean Hs = 0.4–0.7 m). Southwest monsoons, which run from May to October, bring greater wave energy to the east coast provinces, with peaks of 0.8–1.2 m occurring during monsoon seasons [8].

Table 2. Summary of oceanographic parameters across Gulf of Thailand regions.

Parameter	Inner Gulf	Eastern Seaboard	Western Gulf	Southern Gulf	Unit
Mean Hs (annual)	0.3–0.5	0.5–0.9	0.5–0.8	0.7–1.0	m
Extreme Hs (50-yr)	1.5–2.0	2.0–2.5	2.5–3.0	3.0–3.5	m
Mean wave period	3–4	4–5	4–6	5–6	s
Tidal range (spring)	2.5–3.0	1.6–2.1	1.5–2.2	1.0–1.5	m
Mean current velocity	0.2–0.3	0.3–0.5	0.2–0.4	0.3–0.5	m/s
Mean GHI	4.85–4.92	4.95–5.29	4.78–5.02	4.65–4.78	kWh/m^2/d

Note: Hs = significant wave height; GHI = Global Horizontal Irradiance. Values represent typical ranges at 2–5 km offshore. Data derived from ERA5 reanalysis (2019–2023) validated against in-situ observations [8,9,39,40].

Thailand's geographical position within the tropical zone (approximately between 6–14° N) makes it possible to get adequate radiation from the sun for the entire year. Among the nine surveyed provinces, the ones situated on the east coast have shown maximum levels of irradiation on average, with the values for Rayong standing at 5.29 kWh/m^2/day and for Chonburi, 5.15 kWh/m^2/day. The inner gulf provinces display relatively lower levels of GHI (around 4.85–4.92 kWh/m^2/day) due to greater atmospheric humidity and higher aerosol concentrations from the Bangkok area [41].

2.3. Grid Infrastructure and Industrial Context

Grid connectivity represents a critical factor for N-FPV project viability, as submarine cable costs and electrical losses increase substantially with distance from shore-based interconnection points. The nine study provinces exhibit varying levels of electrical infrastructure development, with the eastern seaboard provinces benefiting from extensive grid reinforcement associated with the Eastern Economic Corridor (EEC) industrial development [42]. Rayong and Chonburi provinces host Thailand's highest concentration of high-voltage transmission infrastructure along the coastline, including multiple 230 kV and 115 kV substations within 20 km of potential N-FPV deployment zones. The Map Ta Phut industrial complex in Rayong alone represents over 2,850 MW of connected industrial load, providing substantial local demand for renewable electricity through corporate power purchase agreements [37]. It is acknowledged that industrial electricity demand (C8) was proxied using provincial aggregate loads due to the unavailability of harmonized coastal-belt or nearshore-adjacent industrial datasets. As a result, provinces with large inland industrial bases—particularly in the EEC—may receive optimistic demand scores that do not necessarily reflect coastal offtake concentration within feasible nearshore buffers. This proxy limitation is tested through a demand-reduction sensitivity analysis in Section 4.5. Furthermore, grid proximity values (C7) in the following tables represent straight-line Euclidean distances to the nearest high-voltage interconnection point; actual submarine cable routing distances are typically 1.3–2.0× longer due to seafloor bathymetry constraints, shipping lane avoidance, and regulatory exclusion zones. The sensitivity of rankings to route-adjusted cable distances is explicitly tested in Section 4.5. Developer-level assessments should validate these assumptions with site-specific bathymetric surveys and EGAT/PEA interconnection studies.

3. Methodology

This study employs an integrated multi-criteria decision analysis (MCDA) framework combining the Analytic Hierarchy Process (AHP) for subjective criteria weighting—supplemented by entropy-based objective weighting for validation—with the Technique for Order Preference by Similarity to Ideal Solution (TOPSIS) for provincial ranking, followed by techno-economic assessment (TEA) of priority locations. The methodology comprises six phases: (1) data acquisition and processing; (2) evaluation criteria definition and inter-criteria correlation analysis; (3) AHP-based weight elicitation with entropy validation; (4) TOPSIS provincial ranking; (5) multi-method robustness testing; and (6) techno-economic evaluation with Monte Carlo uncertainty propagation. **Figure 2** illustrates the integrated research framework.

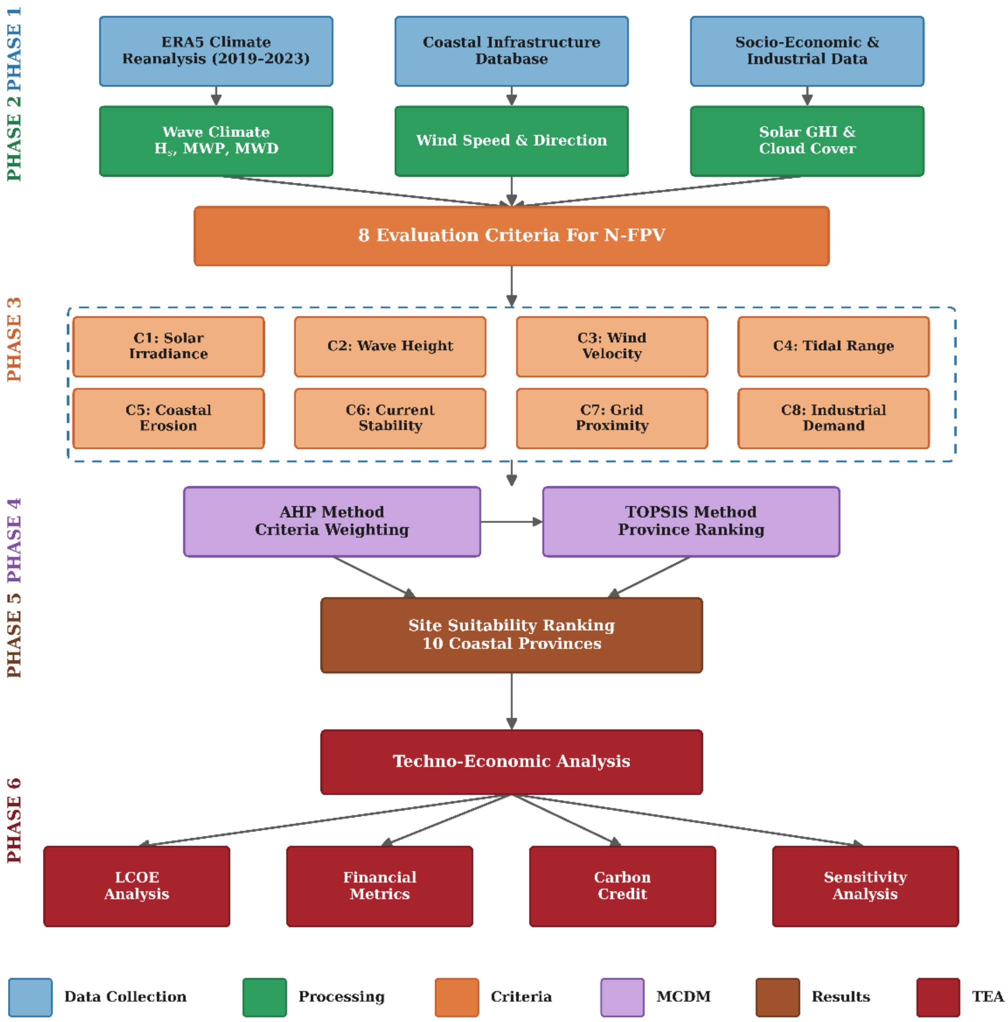

Figure 2. Research methodology framework illustrating the integration of AHP criteria weighting, entropy validation, TOPSIS provincial ranking, multi-method robustness testing, and techno-economic analysis components.

3.1. Data Acquisition and Processing

The environmental and technical datasets were collected from various sources to describe the nearshore environment in the nine study provinces. The main source data consisted of: (1) ERA5 atmospheric reanalysis data from the Copernicus Climate Data Store during the period 2019–2023; (2) HYCOM ocean model outputs providing information on currents' velocities; (3) the Thailand Marine Department's tidal range database; (4) inventories of coast protection structures in Thailand from government agencies in the country; and (5) socio-economic data from the province statistics offices. ERA5 reanalysis data serve as the basis for describing wave climate, wind regime, and solar radiation in the Gulf of Thailand [43–45]. The wave characteristics included significant wave height (Hs), mean wave period (MWP), and mean wave direction (MWD), which were collected at a resolution of 0.5° × 0.5° with a 1-h step. Atmospheric data such as wind speed components at the 10 m height level (u10, v10), downward shortwave radiation (ssrd), and cloudiness (tcc) were retrieved at 0.25° × 0.25° resolution. This five-year period covers annual fluctuations in climate patterns caused by monsoon winds and El Niño–Southern Oscillation (ENSO) influence. **Table 3** summarizes the ERA5 dataset used.

Table 3. ERA5 reanalysis variables used in N-FPV pre-screening.

Variable	ERA5 Code	Resolution	Unit	Temporal	Criterion
Significant wave height	swh	0.5° × 0.5°	m	Hourly	C2
Mean wave period	mwp	0.5° × 0.5°	s	Hourly	Support
10-m U wind component	u10	0.25° × 0.25°	m/s	Hourly	C3
10-m V wind component	v10	0.25° × 0.25°	m/s	Hourly	C3
Surface solar radiation	ssrd	0.25° × 0.25°	J/m^2	Hourly	C1

Note: Data period 2019–2023 (5 years). ssrd converted to GHI (kWh/m2/day) using: GHI = ssrd × 24/3,600,000.

Spatial resolution limitation: ERA5's native resolution (0.25°–0.5°, corresponding to approximately 28–56 km grid spacing) is too coarse to resolve fine-scale nearshore features such as headland diffraction, harbor-induced sheltering, or localized bathymetric effects that can produce substantial local variability within a single province. The bilinear interpolation applied to increase effective resolution to 0.05° (~5.5 km) improves spatial representation for provincial comparison but does not create new physical information beyond ERA5's native resolution. Accordingly, the interpolated fields are used for relative macro-screening among provinces rather than for absolute engineering design parameters, and the results cannot support claims about practical siting superiority at the coastal belt scale. High-resolution nested wave modeling (e.g., Simulating WAves Nearshore (SWAN) or MIKE21) would be required for site-specific engineering characterization.

To operationalize the nearshore definition at the provincial scale, each coastal province was represented by gridded nearshore cells within a 2–10 km coastal buffer and depths of 5–30 m. For every criterion derived from spatial fields (GHI, Hs, wind, and current), values were first extracted at all eligible nearshore cells, and then summarized using the provincial median together with the inter-quartile range (IQR). The median was used in TOPSIS to reduce bias from localized extremes, while the IQR is reported as an indicator of intra-provincial heterogeneity. It is stressed that provincial medians mask significant spatial variability—a single province may contain both highly suitable and unsuitable zones—and therefore the rankings should not imply coastal uniformity. Developers must resolve within-province variability through GIS micro-siting before selecting specific deployment polygons. Nearshore wave transformation was applied to account for shoaling, refraction, and depth-induced breaking effects using Equation (1):

$$H_{s,nearshore} = K_s \times K_r \times K_d \times H_{s,offshore} \quad (1)$$

Here, K_s refers to the shoaling coefficient (normally in the range 0.9–1.1), K_r refers to the refraction coefficient (0.85–1.0), while K_d is the depth-dependent wave breaking coefficient (0.8–1.0). Transformation factors were determined using General Bathymetric Chart of the Oceans (GEBCO) bathymetry data [46] through linear wave theory, and compared with available in-situ measurements from wave buoys from the Royal Thai Navy [47]. This first-order transformation factor can only distinguish among provinces based on suitability scores, as it is sufficient for screening at the provincial scale but inadequate for differentiating those that have very similar suitability scores. This current transformation cannot be assumed to provide high-fidelity hydrodynamics; instead, it aims at improving relative comparability among provinces during screening. The ERA5 reanalysis data were validated using available in-situ measurement data to assess their accuracy and any bias. **Table 4** shows the validation results. Bias correction factors were then used to multiply all ERA5 data.

Table 4. ERA5 data validation against in-situ observations.

Parameter	Reference Stations	R^2	Root Mean Square Error (RMSE)	Mean Bias Error (MBE) (%)	Correction
Significant wave height	4 RTN buoys	0.87	0.18 m	+7.2	×0.93
Wind speed (10 m)	12 TMD stations	0.91	0.65 m/s	−5.2	×1.05
Solar irradiance (GHI)	15 pyranometers	0.93	0.42 kWh/m^2/d	+3.1	×0.97

Note: RTN = Royal Thai Navy; TMD = Thai Meteorological Department. ERA5 wave and wind accuracy in adjacent South China Sea waters has been independently validated [48,49].

3.2. Evaluation Criteria Framework and Inter-Criteria Correlation Analysis

Eight evaluation criteria were selected to characterize N-FPV provincial pre-screening across technical, environmental, and economic dimensions. **Table 5** presents the criteria definitions.

Criteria scope limitations: Several marine-use constraints (shipping lanes, designated fishing grounds, military zones, and sensitive habitats such as seagrass, coral, and mangrove areas) could not be formalized as quantitative criteria at the provincial scale due to a lack of harmonized spatial datasets. In addition, ecological compatibility criteria—including light attenuation effects on primary productivity, benthic habitat disturbance from anchoring systems, and fisheries interference—are recognized as potentially first-order constraints for nearshore FPV feasibility [10,11,53] but cannot be consistently quantified across all nine provinces using existing public datasets. Coastal erosion (C5) was included as the only environmental criterion because it represents the most consistently measured and spatially comparable shoreline indicator available across all study provinces; however, this should not be interpreted as implying that ecological factors are less important. The eight criteria, therefore, represent a techno-economic-environmental screening set, and a GIS-based exclusion layer incorporating marine spatial planning constraints is recommended as a mandatory follow-up step for any top-ranked province.

Table 5. Evaluation criteria for N-FPV provincial pre-screening.

Code	Criterion	Unit	Type	Description	Source
C1	Solar Irradiance	kWh/m^2/d	Benefit (+)	Mean daily GHI determining energy yield	The Copernicus Climate Change Service [39]
C2	Wave Height	m	Cost (−)	Mean Hs affecting structural loads	The Copernicus Climate Change Service [39]
C3	Wind Velocity	m/s	Non-mono*	Mean wind; optimal ~5 m/s for cooling	The Copernicus Climate Change Service [39]
C4	Tidal Range	m	Cost (−)	Spring tidal range affecting mooring	Marine Department [50]
C5	Coastal Erosion	m/yr	Cost (−)	Shoreline retreat rate	Department of Marine and Coastal Resources (DMCR) [51]
C6	Current Velocity	m/s	Cost (−)	Mean tidal current affecting mooring	Hybrid Coordinate Ocean Model (HYCOM) [40]
C7	Grid Proximity	km	Cost (−)	Euclidean distance to grid interconnection	Provincial Electricity Authority (PEA) [42]; Electricity Generating Authority of Thailand (EGAT) [52]
C8	Industrial Demand	MW	Benefit (+)	Provincial aggregate industrial load (proxy)	Thailand Board of Investment (BOI) [37]; PEA [42]

Note: *C3 Wind Velocity exhibits non-monotonic optimality (~5 m/s optimal). Asymmetric transformation applied prior to TOPSIS (see Equation 2).

3.2.1. Inter-Criteria Correlation Analysis

Pearson Correlation Matrix Heatmap with AHP Weights Below Corresponding Criteria is shown in **Figure 3**. Among the absolute correlations, the most significant correlation coefficient value is |r| = 0.68 between C2 (wave height) and C3 (wind velocity), |r| = 0.67 between C7 (grid proximity) and C8 (industrial demand), and |r| = 0.65 between C4 (tidal range) and C5 (coastal erosion). The latter three criterion pairs are marked in yellow borders in **Figure 3**; they come close but fall below the |r| = 0.70 cutoff value used in the MCDA literature as an indicator of redundancy [29,31]. Criterion pair C2–C3 represents wind-wave physics; criterion pair C7–C8 reflects geospatial clustering of grid proximity and industrial demand on the EEC corridor; and criterion pair C4–C5 indicates coastal dynamics of the inner Gulf area. While these high correlations do not imply criterion exclusion in the screening phase, it suggests possible overemphasis when combining the two criterion weights (C2 + C3 = 24.5%, C7 + C8 = 30.7%). This bias is balanced out to some extent by comparing weights obtained via the Entropy Method (Section 3.3).

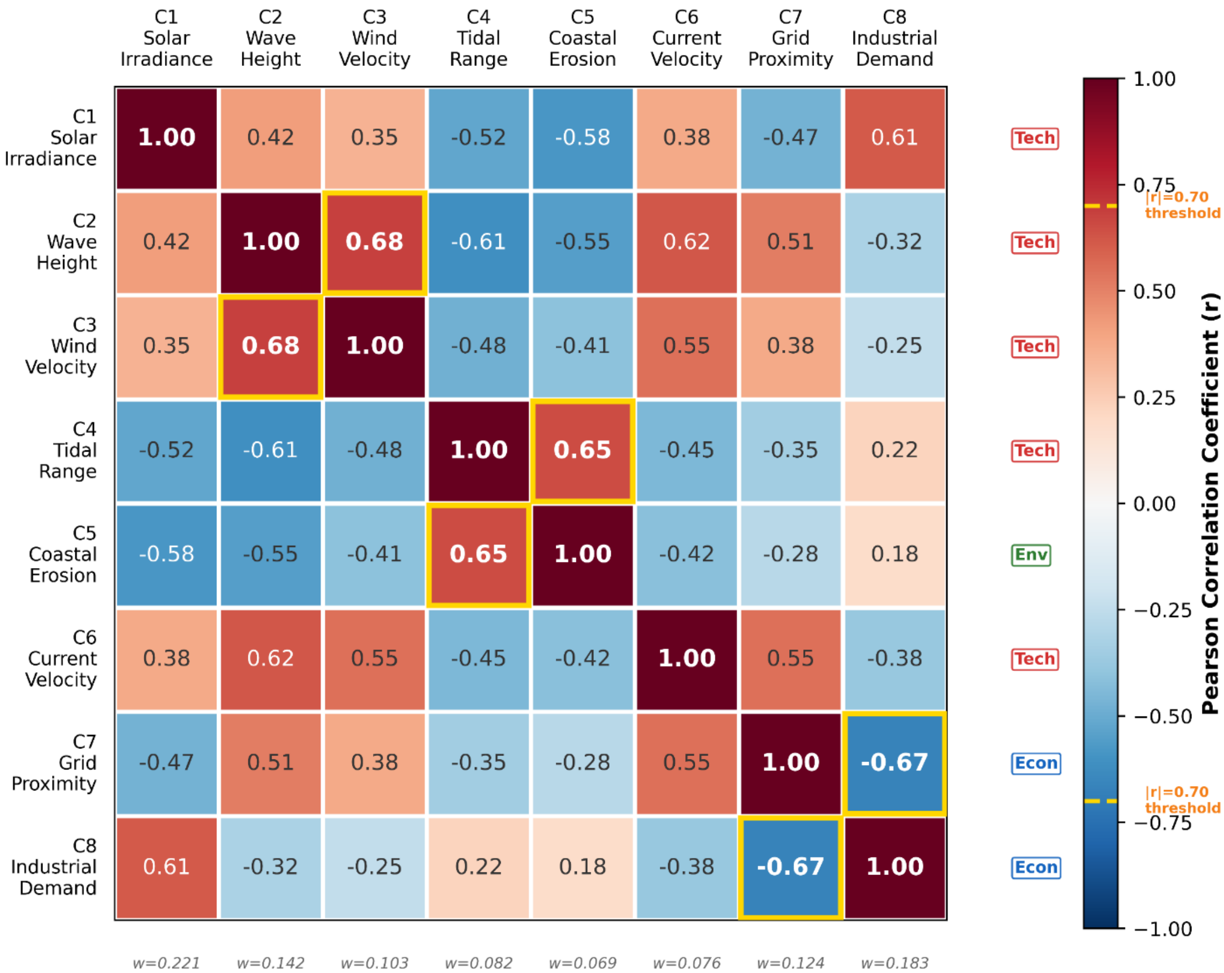

Figure 3. Inter-criteria Pearson correlation heatmap for eight N-FPV evaluation criteria (n = 9 provinces).

Note: Color scale: red = positive, blue = negative correlation. Yellow-bordered cells indicate the three highest pairs (|r| ≥ 0.65). All correlations remain below the |r| = 0.70 redundancy threshold. AHP weights shown below each criterion; category labels: Technical (Tech), Environmental (Env), Economic (Econ).

3.2.2. Asymmetric Wind Velocity Transformation

Wind velocity (C3) exhibits a non-monotonic influence on nearshore FPV feasibility. Moderate winds enhance convective cooling and can improve electrical performance, while high winds increase aerodynamic loads, platform motions, and mooring risk [54]. Because aerodynamic and mooring penalties are more severe at the high-wind tail than at the low-wind tail, the original symmetric absolute-deviation transformation was replaced by an asymmetric penalty function for this revised analysis (Equation 2):

$$C3' = |v_{wind} - v_{optimal}| \times \alpha \quad (2)$$

Let $v_{optimal}$ = 5.0 m/s, where α is set at 1.0 for wind speeds less than or equal to $v_{optimal}$ (low-wind case) and 1.5 for wind speeds greater than $v_{optimal}$ (high-wind case). The 50% greater weighting factor, α = 1.5, for high wind speeds than for optimal wind speeds accounts for the higher penalties for high winds from the standpoint of structural integrity and operational stability than for low winds, which cause only a relatively small decrease in performance [5,38]. This model is more physically realistic than a symmetric function. This first-order model is sufficient for provincial-level screening; however, in GIS-based micrositing, a complete aerodynamic load analysis must be used.

3.3. AHP Criteria Weighting

The criteria weights, which are indicative of the criteria's relative significance in the N-FPV screening process, were established using the Analytic Hierarchy Process (AHP) model proposed by Saaty (1980) [26]. Five experts from the respective domains were invited to provide their judgments in pairs, as presented in **Table 6** below.

Limitation regarding panel composition: Although the expert panel (n = 5) meets the requirements of structured expert judgment analysis, it does not provide comprehensive coverage of the stakeholder groups necessary for evaluating the siting of marine renewable energy projects. For instance, the panel lacks fisheries experts, marine spatial planners, and coastal permit issuers. The omission of such perspectives might lead to systematic biases favoring techno-economic factors over socio-environmental factors. The acceptable level of consistency (CR = 0.053) and high inter-rater agreement (W = 0.71, $p < 0.001$) demonstrated by the five experts do not necessarily imply that a panel with greater diversity in stakeholder perspectives, such as fisheries, communities along the coast, and marine biologists, will reach the same consensus. In future applications, it is recommended to utilize larger expert panels with an explicit Delphi technique-based iterative process to incorporate social and environmental perspectives. Each expert independently generated a paired comparison matrix based on Saaty's fundamental scale of 1 to 9. Aggregation of individual matrices was performed by the geometric mean approach [55]. The resulting matrix yielded λ_{max} = 8.52 and CR = 0.053, which is far below the threshold value of 0.10. Uncertainty associated with the weights derived from AHP was calculated by applying a bootstrap Monte Carlo simulation: each matrix element was varied by ±1 standard deviation, and the weights were recalculated in 1,000 iterations. **Table 7** presents the criteria weights generated by AHP.

Table 6. Expert panel composition for AHP weight elicitation.

ID	Affiliation	Specialization	Experience	Role
E1	University	Marine renewable energy systems	15 years	Technical
E2	University	Coastal and ocean engineering	12 years	Technical
E3	Consulting firm	Energy economics and project finance	10 years	Economic
E4	Government (DMCR)	Environmental impact assessment	8 years	Environment
E5	Industry (FPV developer)	Floating solar project implementation	6 years	Practical

Table 7. AHP-derived criteria weights for N-FPV pre-screening.

Code	Criterion	Weight (w_j)	Weight (%)	95% CI	Rank	Category
C1	Solar Irradiance	0.221	22.1	[0.195, 0.248]	1	Technical
C8	Industrial Demand	0.183	18.3	[0.158, 0.210]	2	Economic
C2	Wave Height	0.142	14.2	[0.121, 0.165]	3	Technical
C7	Grid Proximity	0.124	12.4	[0.105, 0.145]	4	Economic
C3	Wind Velocity	0.103	10.3	[0.085, 0.122]	5	Technical
C4	Tidal Range	0.082	8.2	[0.068, 0.098]	6	Technical
C6	Current Velocity	0.076	7.6	[0.062, 0.092]	7	Technical
C5	Coastal Erosion	0.069	6.9	[0.055, 0.085]	8	Environment
	Total	1.000	100.0			

Note: λmax = 8.52; CI = 0.074; CR = 0.053 < 0.10 (acceptable). Technical = 62.4%; Economic = 30.7%; Environmental = 6.9%. 95% CI from Monte Carlo bootstrap (n = 1,000).

Entropy-Based Objective Weighting Validation

To assess the sensitivity of rankings to the choice of weighting method and reduce reliance on subjective AHP judgments, entropy-based objective weighting was applied as a complementary approach. The Shannon entropy method derives weights purely from the dispersion of criterion values across alternatives, assigning higher weights to criteria with greater discriminatory power [29,31]. Entropy weights (wEj) were computed as:

$$e_j = -k\, \Sigma_i\, p_{ij} \ln(p_{ij}) \quad (3)$$

$$d_j = 1 - e_j \quad (4)$$

$$w^E_j = d_j / \Sigma_j\, d_j \quad (5)$$

where $p_{ij} = x_{ij}/\Sigma_i\, x_{ij}$ is the normalized proportion, and $k = 1/\ln(m)$ is a normalizing constant for $m = 9$ alternatives.

Comparison between AHP and entropy-weighted structures is shown in **Figure 4**. Panel (A) shows clearly that weight distribution differs drastically: AHP ranks C1 Solar Irradiance as the most important criterion (22.1%), while entropy weight gives it the smallest value due to relatively weak variation of GHI coefficient within the region (coefficient of variation is roughly 4%). Entropy weight ranks C8 Industrial Demand (28.2%) and C7 Grid Proximity (24.5%) higher because of the stronger discriminatory power of these factors (**Figure 3**). Panel (B) summarizes these differences. The largest increase in weight is observed for C7 (+12.1%), due to the wider distribution of inter-provincial distance (3–28 km range). Conversely, the largest decrease is observed for C1 (−18.3%). However, when entropy weights were used to perform TOPSIS estimation, Rayong and Chonburi retained first (Ci = 0.762) and second (Ci = 0.698) places, respectively, proving that the Tier-1 ranking results are consistent with an entirely different approach to assigning weights. Ranking reversals took place only in Tier-3 provinces (7–9th places), which does not affect the findings of this study in any way.

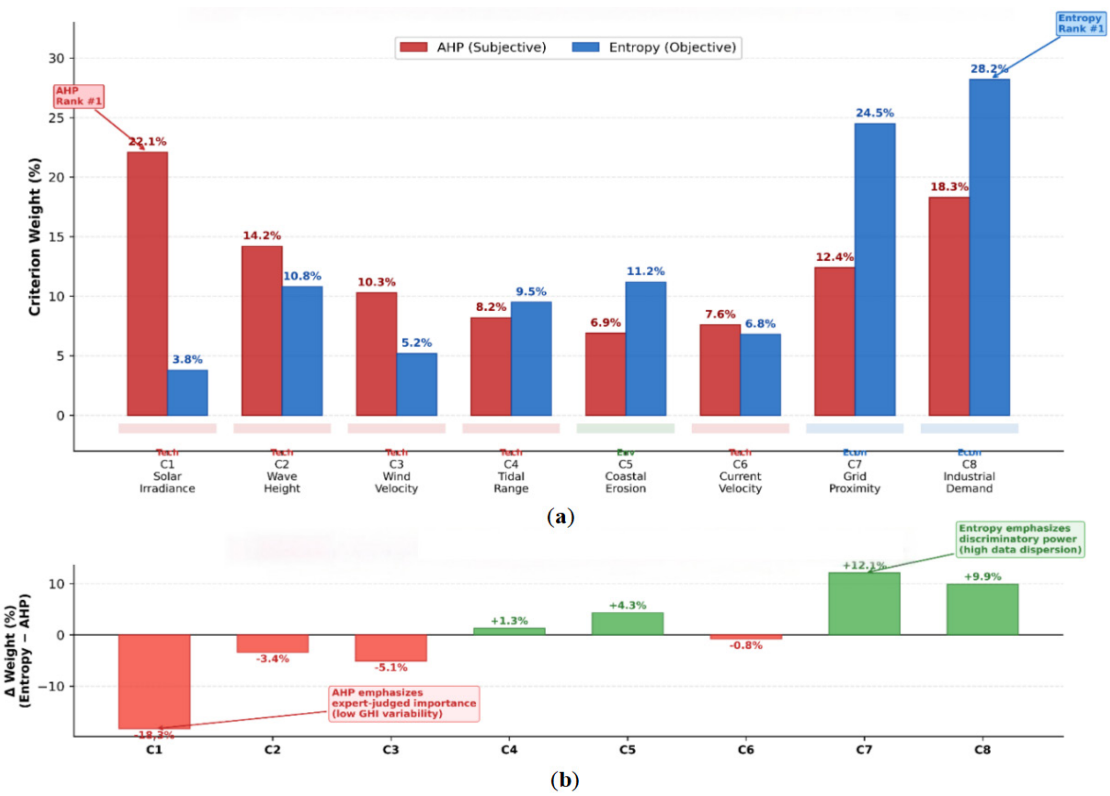

Figure 4. Comparison of AHP (subjective, red) and entropy (objective, blue) criteria weights. (**a**) Grouped bar chart with percentage values annotated; category labels shown at the bottom. (**b**) Weight difference (Entropy − AHP): green = entropy higher, red = AHP higher; interpretation annotations indicate the contrasting weighting philosophies.

3.4. TOPSIS Provincial Ranking

The TOPSIS technique was used to rank nine coastal provinces based on the similarity of their N-FPV attributes to the ideal solution [25]. A decision matrix X = [xij] was established with m = 9 alternatives (provinces) and n = 8 criteria. The vector normalization technique was utilized in normalizing the decision matrix (Equation 6):

$$r_{ij} = x_{ij}/\sqrt{(\Sigma_i\, x_{ij}^2)} \tag{6}$$

The weighted normalized decision matrix V = [v_{ij}] was computed using AHP-derived criteria weights (Equation 7):

$$v_{ij} = w_j \times r_{ij} \tag{7}$$

Positive ideal (A^+) and negative ideal (A^-) solutions were determined based on the criterion type. Euclidean distances were calculated using Equation (8), and the relative closeness coefficient C_i was computed using Equation (9):

$$D_i^+ = \sqrt{(\Sigma_j\, (v_{ij} - A_j^+)^2)} \text{ and } D_i^- = \sqrt{(\Sigma_j\, (v_{ij} - A_j^-)^2)} \tag{8}$$

$$C_i = D_i^-/(D_i^+ + D_i^-) \tag{9}$$

where $C_i \in [0, 1]$, with higher values indicating greater macro-screening suitability for N-FPV.

3.5. Techno-Economic Assessment

A techno-economic analysis was performed for priority provinces identified through TOPSIS ranking to evaluate indicative financial viability under Thai market conditions. Because TEA parameters for nearshore FPV remain scarce in Thailand, cost and performance assumptions were triangulated from (i) marine FPV pilot reports in Asia, (ii) offshore FPV literature, and (iii) local PV EPC benchmarks. This hybridization is necessary for first-order feasibility screening but introduces uncertainty that is explicitly explored via Monte Carlo simulation and scale sensitivity analysis. Annual energy production (AEP) was estimated following IEC 61724-1 methodology (Equation 10):

$$AEP = P_{rated} \times Y_{spec} \tag{10}$$

The performance ratio for nearshore FPV was disaggregated into marine-specific effects: water-surface cooling (+0.5–3%), salt-spray soiling (−3%), submarine cable losses (−2%), and wave-induced motion effects (−3%), resulting in a baseline PR of 0.78 ± 0.05 [38,54,56,57]. LCOE was calculated using the standard discounted cash flow approach (Equation 11):

$$LCOE = (CAPEX \times CRF + OPEX)/AEP \tag{11}$$

where CAPEX is total capital expenditure ($1,200–1,500/kWp for N-FPV) [33,58], CRF is the capital recovery factor (0.0937 at 8% discount rate over 25 years), and Operating Expenditure (OPEX) is annual operating expenditure ($25–35/kWp/year including marine maintenance premium). All monetary values are in 2023-USD.

Monte Carlo uncertainty propagation: To move beyond deterministic single-value LCOE outputs, Monte Carlo simulation (n = 10,000 iterations) was performed for each priority province. Three key parameters were treated as stochastic: CAPEX (triangular distribution: min $1,200, mode $1,350, max $1,500/kWp), performance ratio (normal distribution: $\mu = 0.78$, $\sigma = 0.025$), and annual degradation rate (uniform: 0.4–0.8%/year). The resulting LCOE probability distributions provide 5th/50th/95th percentile values that more accurately reflect the uncertainty inherent in early-stage N-FPV cost estimation.

Scale sensitivity analysis: Because marine balance-of-system costs are highly scale-sensitive, the reference 10 MWp analysis was supplemented with a scale sweep across 5, 10, 20, and 50 MWp plant sizes for Rayong. Scale-dependent CAPEX adjustments were applied using a learning factor: $CAPEX(P) = CAPEX_{ref} \times (P/P_{ref})^{-0.12}$, where the exponent −0.12 reflects marine FPV scale economies observed in literature [33,59]. OPEX was scaled linearly. This sweep demonstrates how LCOE and net present value (NPV) evolve with plant size, providing more informative guidance than a single nominal scenario.

Financial viability was evaluated using net present value (NPV) and internal rate of return (IRR) under three revenue scenarios: (1) conservative Feed-in Tariff (FiT) at $0.08/kWh; (2) base case corporate Power Purchase Agreement (PPA) at $0.12/kWh; and (3) optimistic RE100 buyer scenario at $0.18/kWh [6]. Module degradation of 0.6%/year was applied to the annual AEP. Carbon credit revenue potential was estimated based on avoided CO_2 emissions using Thailand's grid emission factor of 0.499 t CO_2/MWh [60]. Carbon revenue is treated as contingent supplementary upside rather than core project economics, reflecting the immaturity of carbon certification pathways for marine FPV assets and the uncertainty surrounding long-term carbon price trajectories. The financial viability discussion (Section 5.1) is therefore grounded in PPA and FiT revenues, with carbon income presented as an incremental sensitivity parameter rather than a bankable revenue stream.

4. Results

4.1. Environmental Characterization

A further examination of the ERA5 reanalysis dataset for the period 2019–2023 demonstrates marked spatial heterogeneity in environmental conditions in the nine considered provinces. Solar radiation is the greatest on the eastern coast, with the mean daily GHI in Rayong being 5.29 kWh/m^2/day and 5.15 kWh/m^2/day in Chonburi. The inner Gulf provinces have slightly lower GHI values of 4.85–4.92 kWh/m^2/day, whereas the southern Gulf provinces exhibit the least irradiation at 4.65–4.78 kWh/m^2/day. The wave climate analysis confirms the superiority of the eastern coast in terms of mean-state conditions, with mean significant wave height (Hs) varying from 0.48 m in Chonburi to 0.62 m in Chanthaburi, far less than in western Gulf provinces, which include Chumphon (0.85 m) and Phetchaburi (0.72 m). It must be highlighted, though, that mean-state Hs is no guarantee of survivability during extreme weather episodes, and thus Tier-1 provinces must undertake an extreme wave assessment in the FEED stage. **Table 8** presents the entire decision matrix with all criterion values and within-province dispersion measures.

Table 8. Decision matrix for N-FPV provincial pre-screening (raw values with IQR).

Province	C1 GHI (kWh/m^2/d)	C2 Hs (m)	C3 Wind (m/s)	C4 Tide (m)	C5 Eros. (m/yr)	C6 Curr. (m/s)	C7 Grid (km)	C8 Demand (MW)
Rayong	5.29 ± 0.12	0.52 ± 0.08	4.6 ± 0.4	1.8	1.2	0.35 ± 0.05	3	2,850
Chonburi	5.15 ± 0.15	0.48 ± 0.10	4.3 ± 0.5	2.0	1.5	0.32 ± 0.06	5	2,420
Samut Prakan	4.92 ± 0.08	0.38 ± 0.04	4.0 ± 0.3	2.8	3.2	0.28 ± 0.04	8	1,850
Samut Sakhon	4.85 ± 0.10	0.35 ± 0.05	3.8 ± 0.3	2.6	2.8	0.25 ± 0.03	12	1,420
Chanthaburi	5.02 ± 0.14	0.62 ± 0.12	4.8 ± 0.5	1.9	1.8	0.38 ± 0.07	15	680
Trat	4.95 ± 0.18	0.58 ± 0.15	4.5 ± 0.6	1.6	1.4	0.42 ± 0.08	22	320
Phetchaburi	4.88 ± 0.11	0.72 ± 0.14	4.2 ± 0.4	2.2	2.5	0.30 ± 0.05	18	580
Chumphon	4.78 ± 0.16	0.85 ± 0.18	4.9 ± 0.7	1.8	2.2	0.35 ± 0.06	25	450
Songkhla	4.65 ± 0.21	0.92 ± 0.16	5.2 ± 0.8	1.2	1.8	0.45 ± 0.09	28	720

Note: ± values represent inter-quartile ranges (IQR) indicating within-province spatial heterogeneity. Larger IQR values (e.g., Trat Hs ± 0.15 m; Songkhla GHI ± 0.21) indicate provinces where median values are less representative and sub-provincial variability is substantial. C7 and C8 are province-level scalar values without spatial IQR. C5 from DMCR (2023) [51]. C7 = straight-line Euclidean distance; actual cable routes are typically 1.3–2.0× longer. C8 = provincial aggregate industrial load, not coastal-adjacent demand (see demand-proxy sensitivity test in Section 4.5).

The spatial distribution of the two highest-weighted environmental parameters—solar irradiance (C1) and wave height (C2)—is illustrated in **Figure 5** below. In **Figure 5a**, it can be seen that there is a north-to-south difference in Global Horizontal Irradiance (GHI), with the eastern seaboard provinces recording high levels of irradiance compared to the southern provinces. Rayong (5.29 ± 0.12), Chonburi (5.15 ± 0.15 kWh/m^2/day) recorded high irradiance levels, whereas Songkhla recorded low levels of irradiance (4.65 ± 0.21 kWh/m^2/day). **Figure 5b** displays the opposite pattern where there is a relationship between wave height and spatial distribution. Provinces along the inner Gulf recorded the lowest wave heights (Samut Sakhon 0.35 ± 0.05 m), whereas provinces in the southern and western parts had the highest wave heights (Songkhla 0.92 ± 0.16 m). The IQR values given in each graph represent the differences within each province.

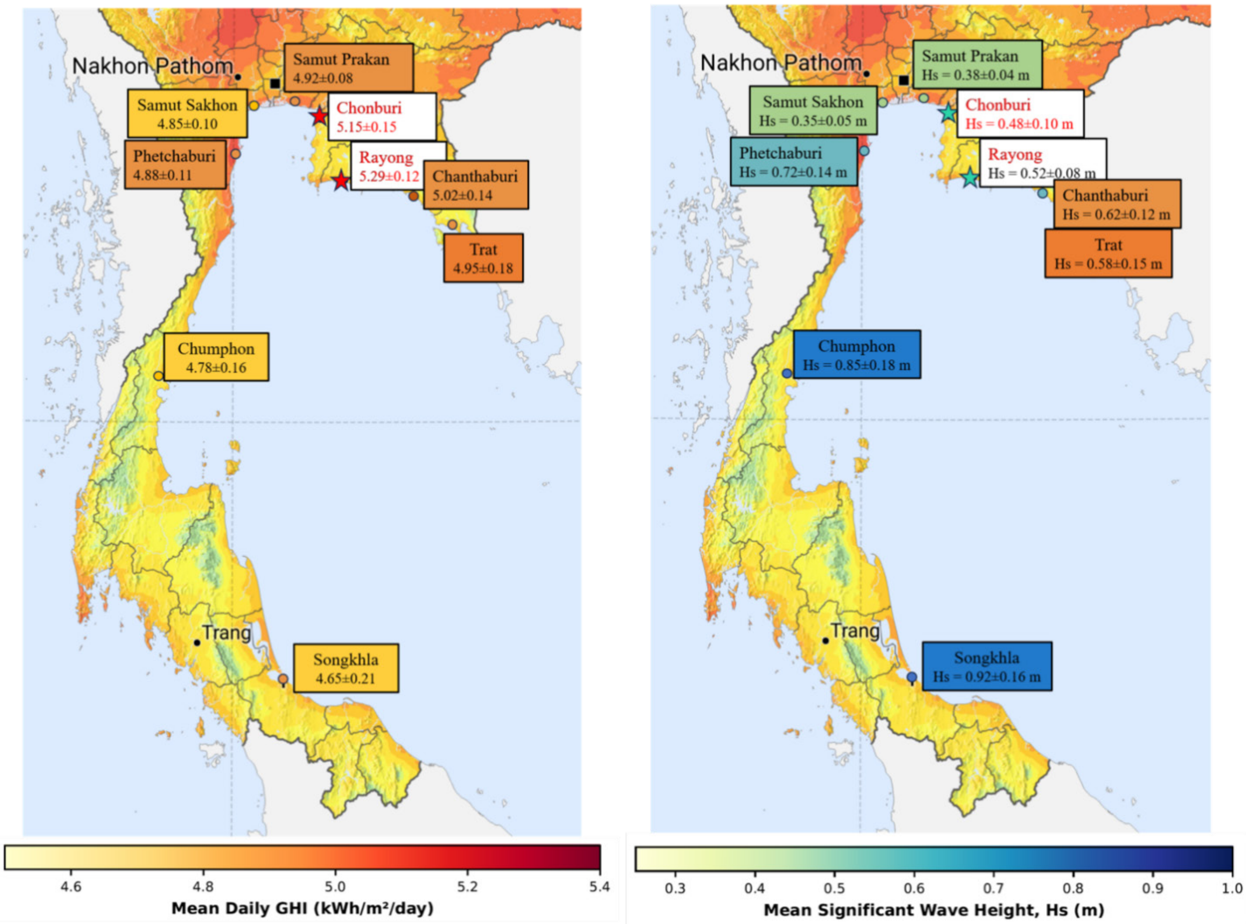

(**a**) (**b**)

Figure 5. Spatial distribution of (**a**) Mean daily global horizontal irradiance (GHI, kWh/m^2/day) and (**b**) Mean significant wave height (Hs, m) across nine Gulf of Thailand coastal provinces.

Note: Values represent provincial nearshore medians ± inter-quartile range (IQR) from ERA5 reanalysis data (2019–2023), bias-corrected against in-situ observations.

4.2. TOPSIS Provincial Ranking Results

TOPSIS technique was used to perform macro-level screening ranking for the nine coastal provinces, shown in **Table 9**. This technique involved the use of criteria weights calculated using the AHP technique (asymmetric wind transformation) in order to calculate closeness coefficients (Ci) ranging between 0.298 and 0.741. Rayong emerged as the leading province with a closeness coefficient of 0.741 due to a high solar radiation (5.29 kWh/m^2/day), medium mean-state waves (Hs = 0.52 m), almost optimal wind speed (4.6 m/s) and strong industrial power proxy requirement (2,850 MW). Second position was achieved by Chonburi with a closeness coefficient of 0.682. Third and fourth positions belonged to Samut Prakan (closeness coefficient = 0.610) and Samut Sakhon (closeness coefficient = 0.524) provinces, which are located along the Gulf coast. The rest of the provinces showed decreasing closeness coefficients, with the lowest one being observed in the province of Songkhla (closeness coefficient = 0.298). **Figure 6** shows a multi-criteria radar graph representing the normalized performance values of the best-ranking four provinces according to all eight criteria. Graphical representation of rankings based on closeness coefficients (Ci) is shown in **Figure 7**.

Table 9. TOPSIS macro-screening results.

Province	D_i^+	D_i^-	C_i	Rank	Tier
Rayong	0.0412	0.1178	0.741	1	Tier-1
Chonburi	0.0486	0.1042	0.682	2	Tier-1
Samut Prakan	0.0598	0.0936	0.610	3	Tier-2
Samut Sakhon	0.0724	0.0796	0.524	4	Tier-2
Chanthaburi	0.0812	0.0685	0.458	5	Tier-2
Trat	0.0876	0.0612	0.411	6	Tier-3
Phetchaburi	0.0924	0.0548	0.372	7	Tier-3
Chumphon	0.0986	0.0492	0.333	8	Tier-3
Songkhla	0.1052	0.0446	0.298	9	Tier-3

Note: Tier-1 (Ci ≥ 0.65): recommended for immediate GIS micro-siting and exclusion mapping. Tier-2 (0.45 ≤ Ci < 0.65): conditional investigation depending on marine-use constraints. Tier-3 (Ci < 0.45): long-term consideration after technology and policy maturation. Rankings are based on mean-state conditions and do not incorporate marine-use exclusion zones (ports, shipping lanes, military areas, conservation micro-sites), extreme metocean events, or ecological constraints. These factors may locally overturn provincial suitability and must be assessed at the project level.

Figure 6. Multi-criteria radar chart comparison of the four highest-ranked provinces.

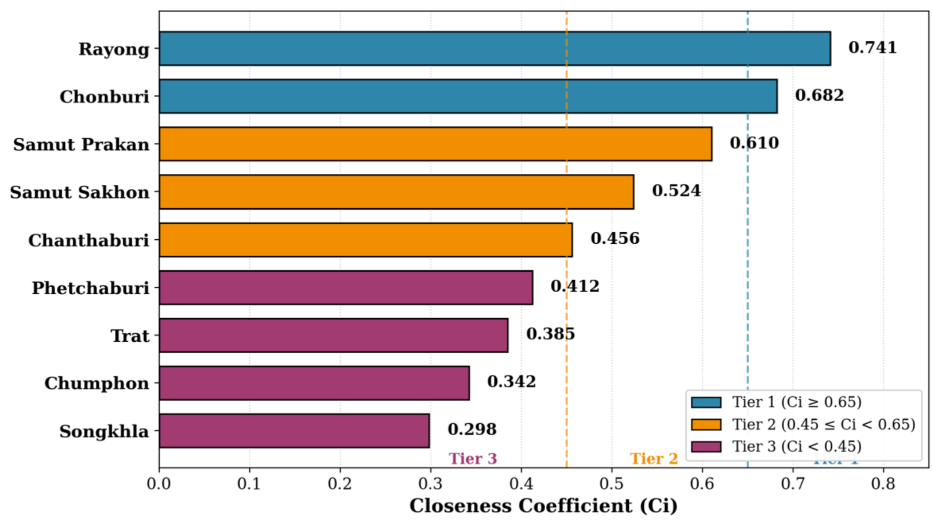

Figure 7. TOPSIS closeness coefficients (C_i) for nine coastal provinces.

4.3. Techno-Economic Assessment

4.3.1. LCOE and Financial Metrics

A comprehensive indicative techno-economic evaluation has been performed on the top three provinces through the use of a 10 MWp reference N-FPV project. It should be noted that the CAPEX and OPEX values assumed in this analysis have been taken from global studies and do not reflect any specific Thai cost structures, supply chain issues, marine insurance requirements, anti-corrosion treatment needs, or regulatory compliance expenses, as illustrated in **Table 10**. Local site feasibility studies based on engineering quotes and permitting practices need to be undertaken before using the above indicative numbers for investment decisions. The probability distributions of the LCOE estimates in the three targeted provinces using Monte Carlo simulations are illustrated in **Figures 8a** (Rayong), **Figure 8b** (Chonburi), and **Figure 8c** (Samut Prakan). The figures show the probability density function (with kernel density estimate) and cumulative distribution functions, with the corresponding P5, P50, and P95 percentiles marked. Threshold lines are also provided for the FiT ($0.08/kWh) and PPA ($0.12/kWh) tariffs. In the case of Rayong, the LCOE values from 99.1% of scenarios will be less than the PPA threshold, reflecting a strong likelihood of financial feasibility under corporate power purchase agreements (PPAs). Similarly, 88.9% and 18.4% probabilities of achieving a PPA in Chonburi and Samut Prakan, respectively, were observed. Notably, no estimated LCOE value in any of the simulated cases will be lower than the FiT threshold level, implying that the mandated procurement mechanism will remain inadequate for N-FPV projects.

Table 10. Indicative techno-economic results for priority N-FPV sites (10 MWp).

Parameter	Rayong	Chonburi	Samut Prakan	Unit
Specific yield	1,535	1,492	1,425	kWh/kWp/yr
Capacity factor	17.5	17.0	16.3	%
Performance ratio	0.80	0.79	0.76	—
AEP	15,350	14,920	14,250	MWh/yr
CAPEX	12.8	13.2	14.2	USD M
OPEX (annual)	0.28	0.30	0.32	USD M/yr
LCOE (deterministic)	0.096	0.102	0.111	USD/kWh
LCOE P5 (Monte Carlo)	0.085	0.090	0.098	USD/kWh
LCOE P50 (Monte Carlo)	0.097	0.103	0.112	USD/kWh
LCOE P95 (Monte Carlo)	0.112	0.119	0.128	USD/kWh

Note: Monte Carlo simulation with n = 10,000 iterations. Stochastic parameters: CAPEX (triangular: $1,200–$1,500/kWp), PR (normal: μ = 0.78, σ = 0.025), degradation (uniform: 0.4–0.8%/yr). P5/P50/P95 represent optimistic/median/conservative LCOE outcomes. All values in 2023-USD.

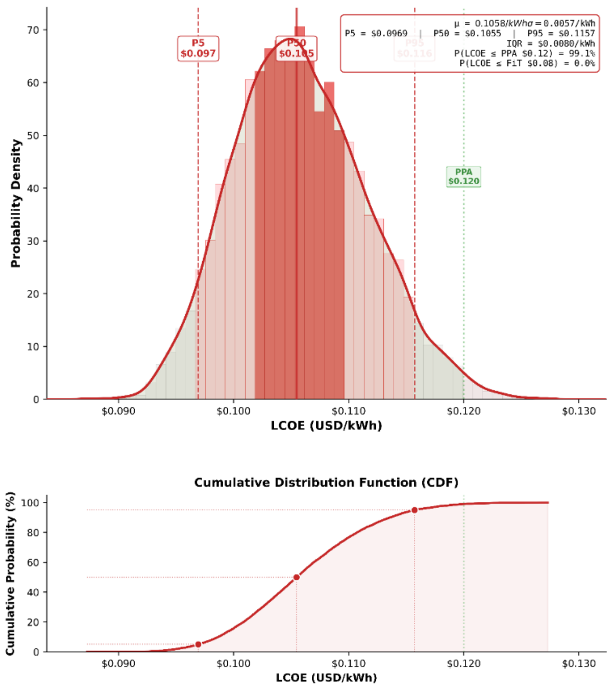

(**a**) Monte Carlo LCOE probability distribution for Rayong (n = 10,000 iterations).

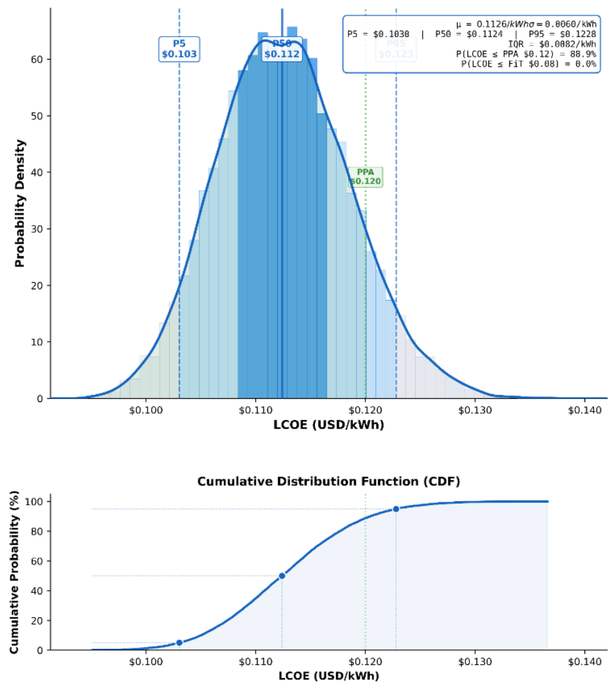

(**b**) Monte Carlo LCOE probability distribution for Chonburi (n = 10,000).

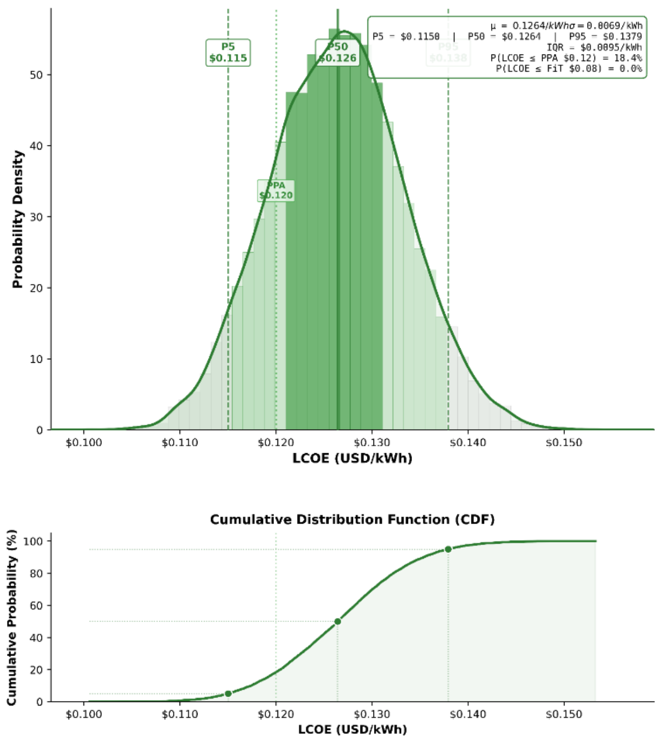

(**c**) Monte Carlo LCOE probability distribution for Samut Prakan (n = 10,000).

Figure 8. Monte Carlo LCOE distributions (n = 10,000) for Rayong, Chonburi, and Samut Prakan, showing histograms with KDE (top) and CDFs (bottom). Dashed lines indicate FiT ($0.08/kWh) and PPA ($0.12/kWh) tariffs.

4.3.2. Scale Sensitivity Analysis

Sensitivity analysis results across the target provinces can be seen in **Figure 9** (Rayong), **Figure 10** (Chonburi), and **Figure 11** (Samut Prakan). **Figure 9** depicts the fact that CAPEX per kWp varies from \$1,391/kWp to \$1,055/kWp across the 5 MWp–50 MWp range, corresponding to the scaling function $CAPEX(P) = CAPEX_{ref} \times (P/P_{ref})^{-0.12}$. **Figure 9b** implies that LCOE falls from \$0.110/kWh to \$0.088/kWh, representing a reduction of 18%, while the PPA threshold (\$0.12/kWh) is exceeded below about 8 MWp for Rayong. NPV of the PPA case changes from slightly positive at 5 MWp (\$0.76M) to significantly positive at 50 MWp (\$24.4M), while NPV remains negative for all scales in the FiT case, according to **Figure 11**. **Figure 9d** shows the increase in IRR from 9.3% to 13.1% under the PPA scenario, exceeding the 8% WACC for all scales above 2 MWp. In the case of Samut Prakan, the PPA scenario gives NPV of more than 0 only above around 30 MWp.

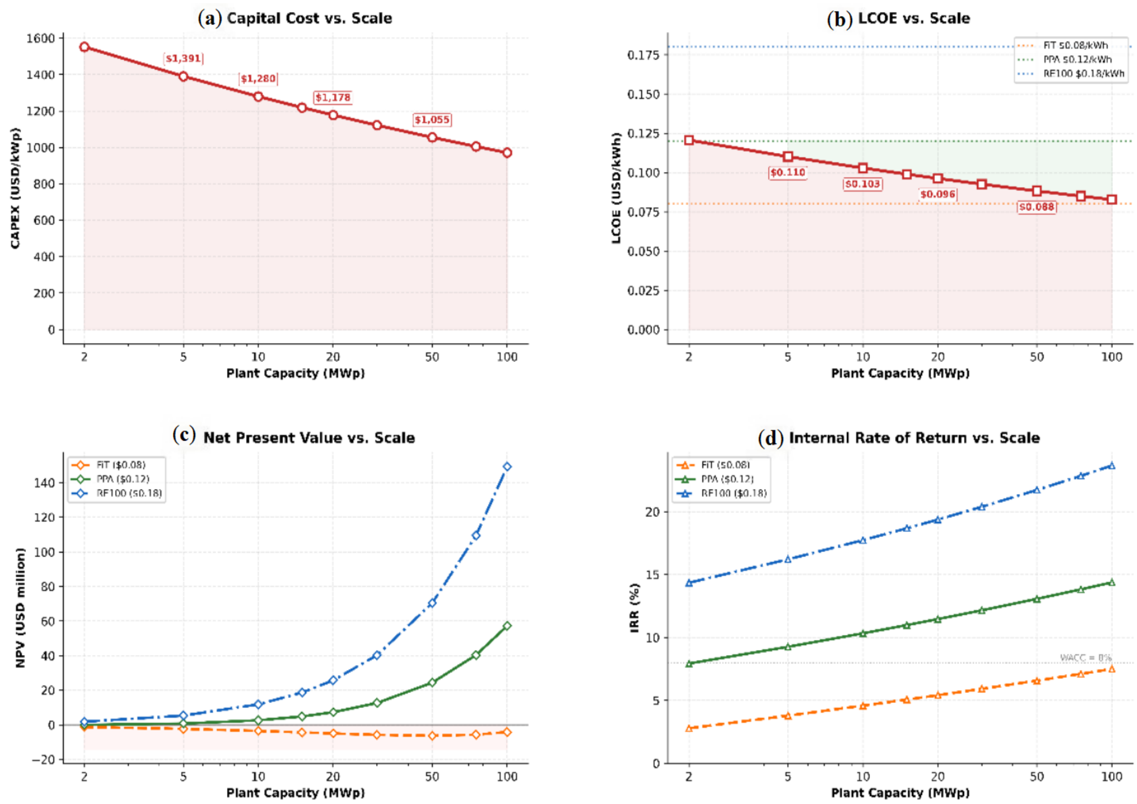

Figure 9. Scale sensitivity analysis for Rayong N-FPV: (**a**) CAPEX per kWp versus plant capacity following CAPEX(P) = \$1,280 × $(P/10)^{-0.12}$; (**b**) LCOE versus plant capacity with FiT, PPA, and RE100 tariff thresholds; (**c**) NPV under three tariff scenarios; (**d**) IRR under three tariff scenarios with WACC = 8% reference line. Plant sizes range from 2 to 100 MWp.

Financial viability was evaluated under three revenue scenarios. Under the FiT scenario at \$0.08/kWh, all three priority sites exhibited negative NPV, indicating that regulated utility procurement mechanisms are insufficient for N-FPV at current cost levels. The PPA scenario at \$0.12/kWh produced positive NPV for Rayong (\$4.8 million, IRR 11.4%) and Chonburi (\$3.5 million, IRR 10.2%). Samut Prakan achieved marginal viability (NPV \$1.8 million, IRR 8.9%). These financial conclusions are presented as indicative screening estimates rather than bankable projections. Local permitting costs, marine insurance premiums, corrosion management requirements, and vessel-based O&M logistics are still represented through literature-based assumptions rather than Thai project data. The tariff thresholds identified should therefore be treated as approximate breakeven indicators that require validation through site-specific engineering and financial due diligence. **Table 11** summarizes the indicative financial metrics under all three revenue scenarios.

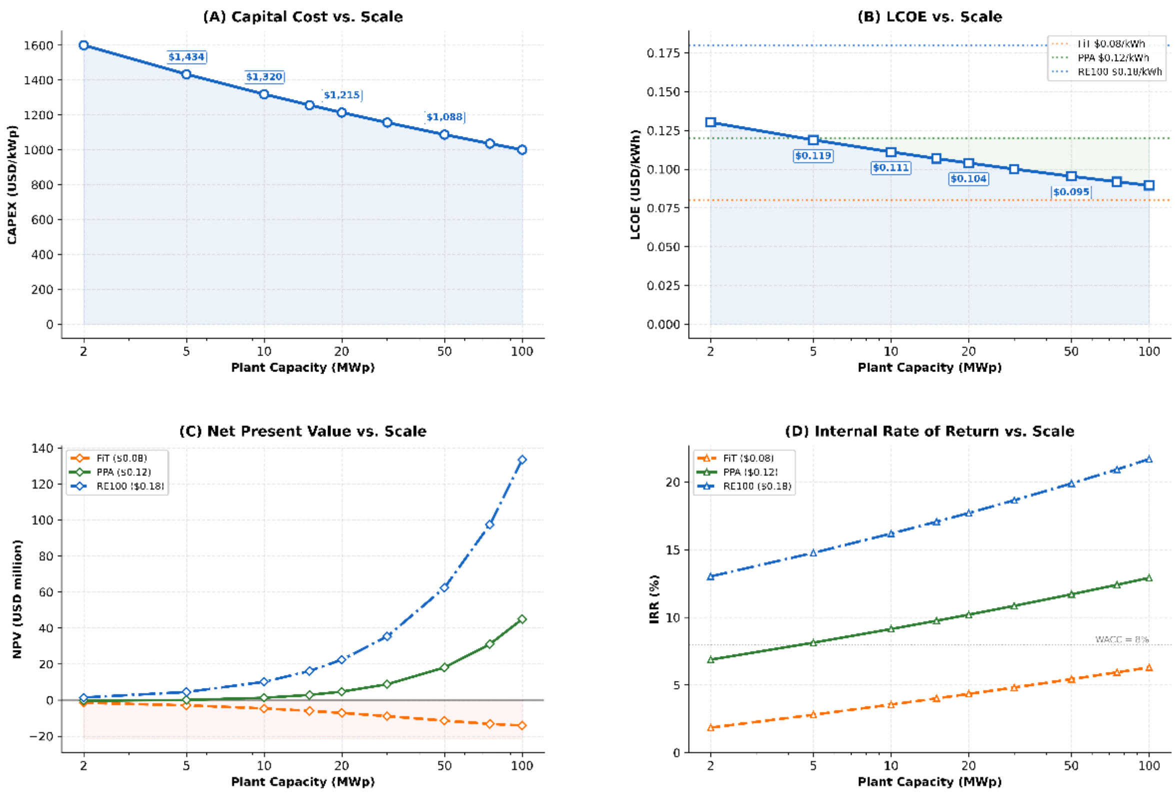

Figure 10. Scale sensitivity analysis for Chonburi N-FPV.

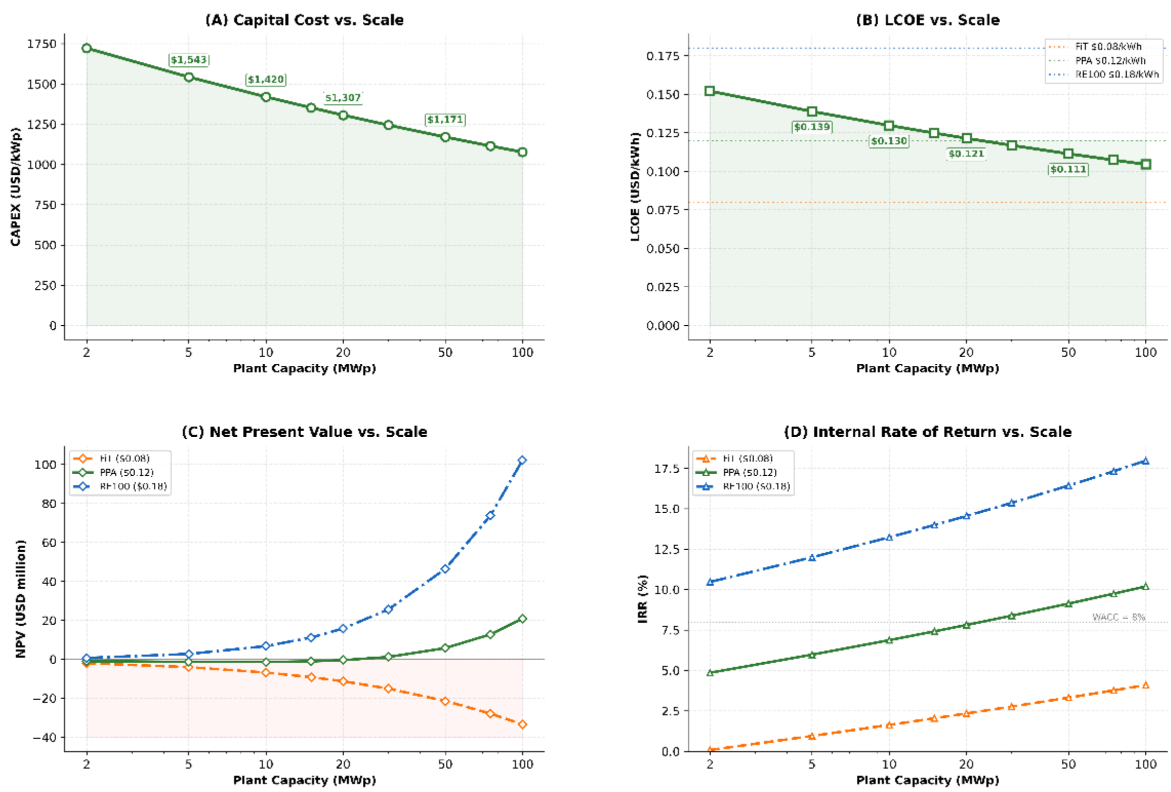

Figure 11. Scale sensitivity analysis for Samut Prakan N-FPV.

Table 11. Indicative financial viability metrics under alternative revenue scenarios.

Province	FiT NPV (USD M)	FiT IRR (%)	PPA NPV (USD M)	PPA IRR (%)	RE100 NPV (USD M)	RE100 IRR (%)
Rayong	−2.4	5.2	4.8	11.4	12.6	18.6
Chonburi	−3.1	4.6	3.5	10.2	10.8	16.8
Samut Prakan	−4.2	3.8	1.8	8.9	8.2	15.2

Note: FiT = $0.08/kWh; PPA = $0.12/kWh; RE100 = $0.18/kWh. NPV at 8% discount rate, 25-year project life.

4.3.3. Carbon Credit Revenue Potential (Contingent Upside)

Carbon credit revenue is presented as contingent supplementary income, not as core project economics. The bankability of carbon revenue for marine FPV depends on successful navigation of monitoring, reporting, and verification (MRV) protocols; certification costs (estimated at 40–60% of gross revenue for small-scale projects); and uncertain long-term carbon price trajectories. Until Thai nearshore FPV projects achieve operational track records and validated Thailand Voluntary Emission Reduction (T-VER) or Gold Standard methodologies, carbon income should not be incorporated into base-case financial models in **Table 12**.

4.4. VIKOR Cross-Validation

To verify the robustness of the TOPSIS rankings, VIKOR cross-validation was performed using the same decision matrix and AHP-derived weights [61,62]. **Table 13** presents the complete VIKOR results.

Table 12. Carbon credit potential (contingent upside, 10 MWp system).

Province	AEP (MWh)	CO_2 Avoided (t)	T-VER (USD 5/t)	Voluntary Carbon Market (VCM) (USD 20/t)	Art. 6 (USD 40/t)
Rayong	15,350	7,660	38,300	153,200	306,400
Chonburi	14,920	7,445	37,225	148,900	297,800
Samut Prakan	14,250	7,111	35,555	142,220	284,440

Note: Net carbon revenue after certification/transaction costs (estimated 50% of gross) would be approximately half these values. Carbon income should be treated as contingent upside, not bankable core revenue.

Table 13. VIKOR cross-validation results (v = 0.5).

Province	S (Utility)	R (Regret)	Q (Compromise)	VIKOR Rank	TOPSIS Rank
Rayong	0.132	0.058	0.000	1	1
Chonburi	0.189	0.068	0.187	2	2
Samut Prakan	0.256	0.082	0.421	3	3
Samut Sakhon	0.318	0.082	0.500	4	4
Chanthaburi	0.445	0.103	0.612	5	5
Trat	0.498	0.103	0.680	6	6
Phetchaburi	0.567	0.110	0.764	7	7
Chumphon	0.652	0.124	0.873	8	8
Songkhla	0.741	0.124	1.000	9	9

Note: Rank order identical for all nine provinces. However, both TOPSIS and VIKOR use the same criteria, the same weights, and the same underlying proxies—this validates ranking algorithm consistency, not the decision model itself. A genuinely independent robustness test using an altered criteria structure is presented in Section 4.5.3.

4.5. Sensitivity and Robustness Analysis

4.5.1. Weight Perturbation Sensitivity

Weight sensitivity analysis applied systematic ±10%, ±20%, and ±30% perturbations to each criterion weight while maintaining normalization constraints. Rayong maintained first place under all perturbation scenarios up to ±22%, which represents the breakpoint at which the C_i gap between Rayong and Chonburi narrows to zero. Industrial Demand (C8) was identified as the most influential factor, with Solar Irradiance (C1) showing the second-highest sensitivity. The tornado diagram in **Figure 12** summarizes the sensitivity of TOPSIS closeness coefficients and NPV to individual parameter perturbations.

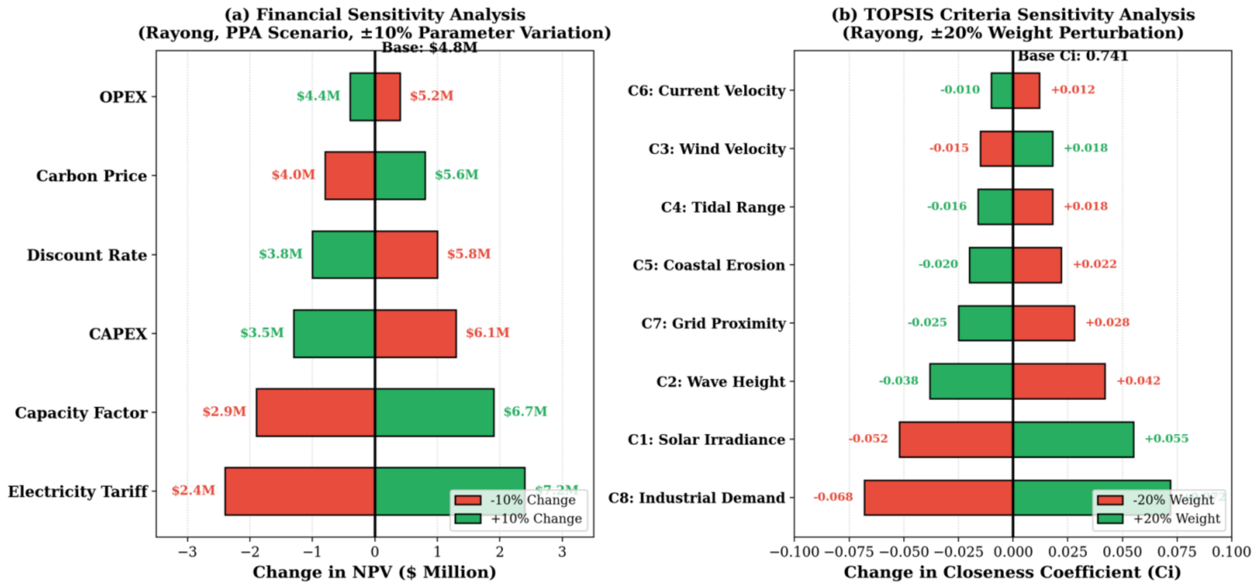

Figure 12. Tornado diagram of sensitivity analysis.

4.5.2. Demand-Proxy Sensitivity Test

Because industrial demand (C8) uses provincial aggregate loads as a proxy—which is structurally favorable to EEC provinces—a conservative sensitivity test reduced C8 scores for Rayong and Chonburi by 30% to simulate lower coastal-adjacent demand. Under this scenario, Rayong retained first place (C_i = 0.718) and Chonburi retained second place (C_i = 0.651), confirming Tier-1 robustness to plausible downward revision of the demand proxy.

4.5.3. Route-Adjusted Grid Distance Sensitivity

To address the concern that straight-line Euclidean distances (C7) understate real cable routing costs, a sensitivity test multiplied all C7 values by 1.5× (representing the midpoint of the 1.3–2.0× routing adjustment range). Under route-adjusted distances, Rayong (adjusted C7 = 4.5 km) retained first place and Chonburi (adjusted C7 = 7.5 km) retained second place. Rank changes occurred only among Tier-3 provinces. This confirms that moderate routing adjustments do not alter the macro-screening hierarchy, though developer-level feasibility must use site-specific bathymetric cable routing.

4.5.4. Altered Criteria Structure Robustness Test

As for the robustness test through VIKOR cross-validation in Section 4.4, it verifies the ranking algorithm but not the decision-making model, because the same set of criteria, weights, and proxies remained intact throughout. In order to conduct the true robustness test, the TOPSIS model was replicated using the new criterion structure, whereby (a) the two pairs of highly correlated criteria (C2–C3 and C7–C8) were combined together using their weighted arithmetic mean according to AHP, thus resulting in six criteria instead of eight; and (b) the criteria weights were recalculated. Using this new six-criteria framework, Rayong retained its leading position (Ci = 0.728), whereas Chonburi continued to rank second (Ci = 0.671). Furthermore, when the economic criteria (C7 and C8) were stripped away, leaving only the six technical/environmental criteria behind, Rayong still ranked first, with Samut Prakan taking up the second spot due to its favorable wave climate, and Chonburi ranking third. This study reveals that the supremacy of Rayong cannot be attributed to the economic criteria, but rather to its technical superiority, whereas the economic factors play a much larger role in Chonburi's ranking.

4.5.5. Financial Sensitivity

Financial sensitivity analysis identified electricity tariff, CAPEX, and capacity factor as primary NPV drivers. When CAPEX increases by 20% and capacity factor decreases by 5% simultaneously (worst-case within observed ranges), Rayong remains viable only above \$0.125/kWh and Chonburi requires \$0.132/kWh. These joint-stress thresholds provide a more realistic bankability envelope than single-parameter sensitivity.

5. Discussion and Conclusions

5.1. Discussion of Findings

The proposed work highlights the application and development of an AHP-TOPSIS integrated multi-criteria decision-making process incorporating entropy-based objective criteria weighting, inter-criteria correlation evaluation, and several robustness tests to conduct systematic N-FPV provincial pre-screening in nine Gulf of Thailand coastal provinces. This paper highlights that Rayong and Chonburi qualify as Tier-1 macro-level screening options, with closeness coefficients of 0.741 and 0.682. These rankings have shown robustness under the established framework due to VIKOR validation, entropy-weighted ranking, demand-proxy sensitivity analysis, grid distance adjusted route sensitivity analysis, and modified criteria structure test. However, it is crucial to note the limits of robustness and what does not necessarily apply: The rankings have been produced based on performance in the mean state environmental condition with respect to techno-economic screening criteria, which may vary under other circumstances and assumptions, such as marine use exclusion areas, extreme metocean conditions, or economic considerations not accounted for in the screening model. The emergence of EEC provinces as Tier-1 candidates owes itself to the coincidence of several positive factors, such as high-quality solar radiation availability, moderate wave climate, high-quality electric grid connectivity, and significant industrial load demand. This is the main empirical finding of this study. However, the significance of industrial load demand is based on provincial-wide figures and not confirmed by the coastal industry's offtake capacity. The demand-proxy sensitivity analysis, as seen in Section 4.5.2, suggests that the Tier-1 rankings hold true for a 30% reduction in industrial demand but future research needs to replace C8 with coastal-industry offtake demand within a specific shoreline strip.

The respective weights of Technical, Economic, and Environmental criteria derived from the AHP technique—namely 62.4%, 30.7%, and 6.9%—are informed by a panel composed of five experts; although limitations arise due to a lack of stakeholder diversity. The low environmental criterion weight must not be misconstrued as a lack of environmental significance; rather, it is due to the nature of the screening process and the limited availability of consistent ecological datasets. For Tier-1 provinces, project-level Environmental Impact Assessments (EIAs) should include the following impacts: light attenuation of primary productivity, seabed disturbance due to anchorages, fishery impact, and habitat displacement. Techno-economic analysis suggests indicative levelized cost of energy (LCOE) values between \$0.096–0.111 per kWh (Monte Carlo P50 \$0.097–\$0.112/kWh) at 10 MWp, rising up to P95 values of \$0.112–0.128/kWh. Scale economies are found by running the simulation scale sweep and finding a decrease in the LCOE between 12–18% for the 5 to 50 MWp capacity range. The finding that FiT (\$0.08/kWh) mechanisms result in negative net present value (NPV) while corporate PPAs (\$0.12/kWh) bring positive NPVs at Rayong and Chonburi suggests that immediate development strategies are dependent on offtake by the private sector. Nonetheless, the above statement must be taken with caution in view of the fact that many important cost factors (maritime insurance, corrosion, O&M logistics at sea, permitting costs) were accounted for using generic literature assumptions instead of Thailand-specific project costs.

5.2. Comparison with International Studies

The LCOE values obtained (\$0.096–0.111/kWh) compare favorably with European assessments reporting \$0.27–\$0.70/kWh for North Sea and Atlantic installations [33] and Mediterranean assessments reporting \$0.16–\$0.24/kWh [63], as well as Mediterranean LCOE mapping showing installation cost as the dominant driver [13]. Life cycle cost analysis of North Sea FPV concepts [20] and global offshore FPV potential assessments projecting LCOE below \$0.06/kWh for Thailand [12] further contextualize these findings. The difference reflects higher tropical solar irradiance, lower wave energy in the semi-enclosed Gulf, and shorter nearshore distances. Unlike temperate-zone assessments, tropical nearshore FPV benefits from smaller seasonal irradiance swings but faces higher biofouling and corrosion rates [10,64]; these contrasting drivers help explain why Thailand can achieve lower LCOE yet still requires premium tariffs for risk compensation. **Table 14** positions the Gulf of Thailand results within the international floating solar literature.

Table 14. Comparison with international nearshore/offshore floating solar assessments.

Study	Location	GHI (kWh/m^2/d)	Mean Hs (m)	LCOE (2023-USD/kWh)	Method
Martinez & Iglesias (2024) [33]	Europe	3.2–4.8	1.5–3.0	0.27–0.70	GIS-MCDA
Gadzanku et al. (2023) [4]	SE Asia	4.5–5.5	0.5–1.5	—	Technical
Liu et al. (2024) [34]	China Coast	3.8–4.5	0.8–1.8	0.12–0.18	AHP-GIS
Magkouris et al. (2023) [63]	Greek Sea	4.5–5.0	0.5–1.5	0.16–0.24	Wave-solar
This study	Gulf of Thailand	4.65–5.29	0.35–0.92	0.096–0.111	AHP-TOPSIS

Note: All LCOE in 2023-USD. EUR values converted at EUR/USD = 1.0813 (ECB 2023).

5.3. Policy Implications

The identification of EEC provinces as priority N-FPV zones supports integration of marine solar into the existing industrial development framework. A differentiated FiT band for nearshore FPV (reflecting higher CAPEX/OPEX than reservoir FPV) could support early-mover projects before corporate PPA volumes scale up. Establishing a "nearshore renewable energy corridor" within EEC waters—co-zoned with shipping and fisheries—would materially reduce project lead times. Despite the Tier-1 prioritization for Rayong and Chonburi, the rankings do not yet internalize explicit marine-use exclusions. In practice, nearshore deployable areas may be substantially reduced by port approach channels (e.g., Map Ta Phut–Laem Chabang corridor), intensive coastal fisheries, naval/security areas, dredging footprints, and sensitive habitats such as seagrass or coral patches. Therefore, Tier-1 provinces should be interpreted as high-potential candidates that require mandatory GIS-based exclusion mapping, stakeholder consultation (including fisheries communities), and site-specific environmental impact assessment before project siting and permitting.

5.4. Limitations

This study has several limitations that bound the interpretation of its findings:

First, the analysis relies on ERA5 reanalysis data at coarse spatial resolution (0.25°–0.5°, approximately 28–56 km grid spacing) that is too coarse for engineering-grade nearshore characterization. Bilinear interpolation does not resolve fine-scale coastal features. The ranking is therefore a macro-screening exercise and cannot support claims about practical siting superiority at the coastal belt scale.

Second, the framework evaluates mean-state environmental conditions. Extreme metocean events—which govern structural survivability, mooring design, and insurance requirements—are not incorporated into the TOPSIS ranking. A province that ranks favorably under mean conditions may be unattractive or unbankable under design storm conditions. Probabilistic extreme value analysis is mandatory before any deployment decision.

Third, the expert panel (n = 5) does not include fisheries, marine spatial planning, or coastal permitting stakeholders, introducing potential bias toward techno-economic criteria. The entropy weighting comparison partially mitigates this concern by showing rank stability under objective weighting, but cannot substitute for broader stakeholder representation.

Fourth, coastal erosion is the only explicit environmental criterion. Ecological compatibility factors—light attenuation, habitat disturbance, fisheries interference, and protected habitat overlap—are not secondary details for nearshore FPV; their exclusion weakens the "suitability" framing. The results should be interpreted as techno-economic pre-screening rather than a comprehensive suitability assessment.

Fifth, industrial demand (C8) uses provincial aggregate loads as a proxy, which is structurally favorable to EEC provinces. The demand-proxy sensitivity test (Section 4.5.2) shows that Tier-1 rankings survive a 30% reduction, but future studies should use coastal-adjacent demand data.

Sixth, marine-use exclusion zones (ports, shipping channels, naval areas, dredging zones, conservation micro-sites) are not explicitly incorporated. These constraints may locally overturn provincial suitability and must be integrated through GIS-based exclusion mapping.

Seventh, the techno-economic assessment assumes a single reference system scale (10 MWp) in the main analysis, supplemented by a scale sweep. CAPEX/OPEX assumptions from international literature may not fully reflect Thai-specific cost structures, marine insurance, corrosion management, or offshore O&M logistics.

Eighth, the moderate correlations between criteria pairs (C2–C3 at r = 0.68; C7–C8 at r = 0.67) imply modest potential for double-counting, though all correlations remain below the |r| = 0.70 redundancy threshold and the entropy weighting comparison confirms rank stability.

5.5. Future Research Directions

An important next stage is the derivation of site polygons from Tier-1 provincial ranking results using GIS-based exclusion mapping of shipping lanes, fishing grounds, military zones, and habitat limitations in the coastal zone of Rayong and Chonburi. Advanced hydrodynamic simulation using nested SWAN or MIKE21 wave models, along with probabilistic extreme value analysis for a 50-year return period of significant wave height (Hs) and wind gust, can be used to facilitate engineering-level site characterization [18,65]. The mooring design must consider the shallow depth and tidal range experienced in the inner Gulf region by utilizing recent findings regarding taut versus catenary mooring options for FPV systems [17,66]. Conducting an environmental impact assessment, including underwater light propagation, water quality, and ecological assessments, is recommended for Tier-1 locations [10,11]. Pilot testing at a scale of 1–5 MWp capacity will not only validate the system but also provide actual performance results to validate the assumptions derived from the literature used in the screening process here.

5.6. Conclusions

This study delivers the first systematic, province-level N-FPV macro-screening for the Gulf of Thailand, integrating AHP-TOPSIS multi-criteria analysis with entropy-based objective weighting validation, VIKOR cross-validation, inter-criteria correlation analysis, and multiple robustness tests, including altered criteria structure experiments. The EEC provinces of Rayong and Chonburi emerge as Tier-1 candidates due to a convergent alignment of solar resource, mean-state wave climate, grid infrastructure, and industrial offtake advantages. The techno-economic analysis establishes that N-FPV viability in Thailand is contingent on corporate PPA offtake at $0.12/kWh or above, not on regulatory feed-in tariffs. Monte Carlo uncertainty propagation yields P50 LCOE values of $0.097–0.112/kWh with P95 uncertainty bounds reaching $0.112–0.128/kWh, indicating that cost outcomes are more uncertain than deterministic point estimates suggest. It is emphasized that the outputs represent provincial pre-screening tiers built on coarse environmental fields, expert-weighted proxies (validated against entropy-based objective weighting), and incomplete exclusion logic. They are not site suitability maps in the practical development sense. The critical next step is converting these macro-screening results into deployable site polygons through mandatory GIS-based exclusion mapping, site-specific extreme-event analysis, ecological impact assessment, and stakeholder engagement—a process that will ultimately determine how much of the 2.7 GW national FPV target is realistically accessible in nearshore marine zones.

Author Contributions

Conceptualization, Y.T.; methodology, K.R. and Y.T.; software, K.R.; validation, K.R. and Y.T.; formal analysis, K.R. and T.D.; data curation, K.R. and T.D.; writing—

original draft preparation, K.R.; writing—review and editing, Y.T.; visualization, K.R.; supervision, Y.T.; project administration, Y.T. All authors have read and agreed to the published version of the manuscript.

Funding

This research received no external funding.

Institutional Review Board Statement

Not applicable. This study did not involve humans or animals; all analyses were conducted using publicly available reanalysis datasets (ERA5, HYCOM) and secondary data from government sources (DMCR, EGAT, PEA, MEA).

Informed Consent Statement

Not applicable.

Data Availability Statement

The ERA5 reanalysis data used in this study are publicly available from the Copernicus Climate Change Service (C3S) Climate Data Store at https://cds.climate.copernicus.eu/. HYCOM ocean current data are freely accessible at https://www.hycom.org. Tide gauge data were obtained from the Marine Department, Ministry of Transport, Thailand (available upon request). Coastal erosion data are available from the Department of Marine and Coastal Resources (DMCR), Thailand, at https://www.dmcr.go.th. All processed datasets and AHP-TOPSIS calculation workbooks supporting the findings of this study are available from the corresponding author upon reasonable request.

Acknowledgements

The authors wish to express sincere appreciation to the Research and Development Institute, Rambhai Barni Rajabhat University, for providing financial support for the publication of this research. The authors gratefully acknowledge Kasetsart University for providing data support and research infrastructure. Deep gratitude is extended to Assoc. Prof. Dr. Yodchai Tiaple for his valuable insights and constructive guidance throughout the development of this study, and to all domain experts who generously contributed their time to the AHP weight elicitation process. This research received no specific grant from any funding agency in the public, commercial, or not-for-profit sectors.

Conflicts of Interest

The authors declare that they have no known competing financial interests or personal relationships that could have appeared to influence the work reported in this paper.

AI Use Statement

During the preparation of this manuscript, the authors used AI tools (ChatGPT and Claude) for language refinement, grammar checking, and figure formatting assistance. No AI tools were used for data analysis, interpretation, or formulation of research conclusions. All outputs were critically reviewed and edited by the authors, who take full responsibility for the content and integrity of the work.

References

[1] International Energy Agency (IEA), 2024. Renewables 2024: Analysis and Forecast to 2030. IEA: Paris, France.

[2] Bai, B., Xiong, S., Ma, X., et al., 2024. Assessment of Floating Solar Photovoltaic Potential in China. Renewable Energy. 220, 119572. DOI: https://doi.org/10.1016/j.renene.2023.119572

[3] Oliveira-Pinto, S., Stokkermans, J., 2020. Marine Floating Solar Plants: An Overview of Potential, Challenges and Feasibility. Maritime Engineering. 173(4), 120–135. DOI: https://doi.org/10.1680/jmaen.2020.10

[4] Gadzanku, S., Joshi, P., Rosenlieb, E., 2023. Enabling Floating Solar Photovoltaic (FPV) Deployment: FPV Technical Potential Assessment for

Southeast Asia. National Renewable Energy Laboratory (NREL): Golden, CO, USA. Available from: https://asiacleanenergyforum.adb.org/wp-content/uploads/2023/06/Sika-Gadzanku.pdf
[5] Djalab, A., Djalab, Z., El Hammoumi, A., et al., 2024. A Comprehensive Review of Floating Photovoltaic Systems: Tech Advances, Marine Environmental Influences on Offshore PV Systems, and Economic Feasibility Analysis. Solar Energy. 277, 112711. DOI: https://doi.org/10.1016/j.solener.2024.112711
[6] Energy Policy and Planning Office (EPPO), 2024. Thailand Power Development Plan 2024–2037 (PDP2024). EPPO: Bangkok, Thailand. Available from: https://www.erc.or.th/th/power-development (in Thai)
[7] Yanagi, T., Takao, T., 1998. Seasonal Variation of Three-Dimensional Circulations in the Gulf of Thailand. La Mer. 36, 43–55. Available from: https://www.sfjo-lamer.org/la_mer/36-2/36-2-1.pdf
[8] Aschariyaphotha, N., Wongwises, P., Wongwises, S., et al., 2008. Simulation of Seasonal Circulations and Thermohaline Variabilities in the Gulf of Thailand. Advances in Atmospheric Sciences. 25, 489–506. DOI: https://doi.org/10.1007/s00376-008-0489-3
[9] Saramul, S., Ezer, T., 2014. On the Dynamics of Low Latitude, Wide and Shallow Coastal System: Numerical Simulations of the Upper Gulf of Thailand. Ocean Dynamics. 64, 557–571. DOI: https://doi.org/10.1007/s10236-014-0703-z
[10] Benjamins, S., Williamson, B., Billing, S.L., et al., 2024. Potential Environmental Impacts of Floating Solar Photovoltaic Systems. Renewable and Sustainable Energy Reviews. 199, 114463. DOI: https://doi.org/10.1016/j.rser.2024.114463
[11] Wu, S., Jiang, N., Zhang, S., et al., 2024. Discussion on the Development of Offshore Floating Photovoltaic Plants, Emphasizing Marine Environmental Protection. Frontiers in Marine Science. 11, 1336783. DOI: https://doi.org/10.3389/fmars.2024.1336783
[12] Rodríguez-Gallegos, C.D., Gandhi, O., Sun, H., et al., 2025. Global Assessment of Offshore Floating Photovoltaics: Technical Potential, Cost Competitiveness, and Deployment Pathway. Energy and Environmental Science. 18, 10537–10562.
[13] Martinez, A., Iglesias, G., 2024. Floating Solar Photovoltaics in the Mediterranean Sea: Mapping and Sensitivity Analysis of the Levelised Cost of Energy. Journal of Cleaner Production. 467, 142983. DOI: https://doi.org/10.1016/j.jclepro.2024.143534
[14] Karipoğlu, F., Koca, K., İlbahar, E., 2024. Convenient Site Selection of a Floating PV Power Plant in Türkiye by Using GIS-Fuzzy Analytical Hierarchy Process. Environmental Science and Pollution Research. 31, 23193–23210. DOI: https://doi.org/10.1007/s11356-024-32470-3
[15] Islam, M.R., Aziz, M.T., Alauddin, M., et al., 2024. Site Suitability Assessment for Solar Power Plants in Bangladesh: A GIS-Based AHP and MCDA Approach. Renewable Energy. 220, 119595. DOI: https://doi.org/10.1016/j.renene.2023.119595
[16] Grace, C.A., Soundranayagam, J.P., Promilton, A.J., et al. 2025. Integrating Remote Sensing and Geospatial-Based Comprehensive Multi-Criteria Decision Analysis Approach for Sustainable Coastal Solar Site Selection in Southern India. ISPRS International Journal of Geo-Information. 14(10), 377. DOI: https://doi.org/10.3390/ijgi14100377
[17] Du, J., Zhang, D., Zhang, Y., et al., 2024. Design and Comparative Analysis of Alternative Mooring Systems for Offshore Floating PV Arrays in Ultra-Shallow Water with Significant Tidal Range. Ocean Engineering. 302, 117649. DOI: https://doi.org/10.1016/j.oceaneng.2024.117649
[18] Li, H., Jiang, Q., Zhang, D., et al., 2024. Hydrodynamic Analysis of Marine Floating Photovoltaics under the Influence of Seabed Topography and Coastlines. Ocean Engineering. 314, 119708. DOI: https://doi.org/10.1016/j.oceaneng.2024.119708
[19] Srinivasan, C.V.C., Soori, P.K., Ghaith, F.A., 2024. Techno-Economic Feasibility of the Use of Floating Solar PV Systems in Oil Platforms. Sustainability. 16(3), 1039. DOI: https://doi.org/10.3390/su16031039
[20] Bru, J., Seland, T.S., Dai, J., et al., 2025. Life Cycle Cost Analysis of an Offshore Floating Photovoltaic Concept in the North Sea. Renewable Energy. 249, 122981. DOI: https://doi.org/10.1016/j.renene.2025.122981
[21] López, M., Claus, R., Soto, F., et al., 2024. Advancing Offshore Solar Energy Generation: The HelioSea Concept. Applied Energy. 359, 122710. DOI: https://doi.org/10.1016/j.apenergy.2024.122710
[22] Gao, X., Guo, J., 2024. Analysis and Research on the Hydrodynamic Performance of Offshore Floating Photovoltaic Systems under Large Tidal Varia-

tions. Journal of Physics: Conference Series. 2865, 012002. DOI: https://doi.org/10.1088/1742-6596/2865/1/012002

[23] Rocha, S.M.G., Armstrong, A., Thackeray, S.J., et al., 2024. Environmental Impacts of Floating Solar Panels on Freshwater Systems and Their Techno-Ecological Synergies. Environmental Research: Infrastructure and Sustainability. 4(4), 042002. DOI: https://doi.org/10.1088/2634-4505/ad8e81

[24] Zhang, C., Dai, J., Ang, K.K., et al., 2024. Development of Compliant Modular Floating Photovoltaic Farm for Coastal Conditions. Renewable and Sustainable Energy Reviews. 190, 114084. DOI: https://doi.org/10.1016/j.rser.2023.114084

[25] Hwang, C.L., Yoon, K., 1981. Multiple Attribute Decision Making. Springer: Berlin/Heidelberg, Germany.

[26] Saaty, T.L., 1980. The Analytic Hierarchy Process: Planning, Priority Setting, Resource Allocation. McGraw-Hill: New York, NY, USA.

[27] Manolache, M., Manolache, A.I., Andrei, G., 2025. Floating Solar Energy Systems: A Review of Economic Feasibility and Cross-Sector Integration with Marine Renewable Energy, Aquaculture and Hydrogen. Journal of Marine Science and Engineering. 13(8), 1404. DOI: https://doi.org/10.3390/jmse13081404

[28] Abdel-Basset, M., Gamal, A., Chakrabortty, R.K., et al., 2021. A New Hybrid Multi-Criteria Decision-Making Approach for Location Selection of Sustainable Offshore Wind Energy Stations: A Case Study. Journal of Cleaner Production. 280, 124462. DOI: https://doi.org/10.1016/j.jclepro.2020.124462

[29] Shao, M., Han, Z., Sun, J., et al., 2020. A Review of Multi-Criteria Decision Making Applications for Renewable Energy Site Selection. Renewable Energy. 157, 377–403. DOI: https://doi.org/10.1016/j.renene.2020.04.137

[30] Demir, A., Dinçer, A.E., Yılmaz, K., 2024. A Novel Procedure for the AHP Method for Site Selection of Solar PV Farms. International Journal of Energy Research. 2024(1), 5535398. DOI: https://doi.org/10.1155/2024/5535398

[31] Deveci, M., Cali, U., Pamucar, D., 2021. Evaluation of criteria for site selection of solar photovoltaic (PV) projects using fuzzy logarithmic additive estimation of weight coefficients. Energy Reports. 7, 8805–8824. DOI: https://doi.org/10.1016/j.egyr.2021.10.104

[32] Haas, J., Khalighi, J., de la Fuente, A., et al., 2020. Floating Photovoltaic Plants: Ecological Impacts Versus Hydropower Operation Flexibility. Energy Conversion and Management. 206, 112414. DOI: https://doi.org/10.1016/j.enconman.2019.112414

[33] Martinez, A., Iglesias, G., 2024. Mapping of the Levelised Cost of Energy from Floating Solar PV in Coastal Waters of the European Atlantic, North Sea and Baltic Sea. Solar Energy. 279, 112809. DOI: https://doi.org/10.1016/j.solener.2024.112809

[34] Liu, G., Guo, J., Peng, H., et al., 2024. Review of Recent Offshore Floating Photovoltaic Systems. Journal of Marine Science and Engineering. 12(11), 1942. DOI: https://doi.org/10.3390/jmse12111942

[35] Di Grazia, S., Tina, G.M., 2023. Optimal Site Selection for Floating Photovoltaic Systems Based on GIS and MCDA: A Case Study. Energy Sources, Part A. 43(1), 2167999. DOI: https://doi.org/10.1080/14786451.2023.2167999

[36] Sojisuporn, P., Morimoto, A., Yanagi, T., 2010. Seasonal Variation of Sea Surface Current in the Gulf of Thailand. Coastal Marine Science. 34(1), 91–102.

[37] Board of Investment (BOI), 2023. Thailand's Eastern Economic Corridor: Investment Opportunities in Targeted Industries. Thailand Board of Investment: Bangkok, Thailand.

[38] Jiang, Z., Dai, J., Saettone, S., et al., 2023. Design and Model Test of a Soft-Connected Lattice-Structured Floating Solar Photovoltaic Concept for Harsh Offshore Conditions. Marine Structures. 90, 103426. DOI: https://doi.org/10.1016/j.marstruc.2023.103426

[39] The Copernicus Climate Change Service (C3S), 2025. ERA5 Hourly Data on Single Levels from 1940 to Present. Available from: https://cds.climate.copernicus.eu/datasets/reanalysis-era5-single-levels?tab=overview (cited 1 December 2025).

[40] Hybrid Coordinate Ocean Model (HYCOM), 2023. HYCOM + NCODA Global 1/12° Analysis. Available from: https://www.hycom.org/dataserver/gofs-3pt0/analysis (cited 1 December 2025).

[41] Janjai, S., Pankaew, P., Laksanaboonsong, J., 2009. A Model for Calculating Hourly Global Solar Radiation from Satellite Data in the Tropics. Applied Energy. 86(9), 1450–1457. DOI: https://doi.org/10.1016/j.apenergy.2009.02.005

[42] Provincial Electricity Authority (PEA), 2023. An-

nual Statistics Report 2023: Electricity Consumption by Sector and Region. Provincial Electricity Authority: Bangkok, Thailand.

[43] Hersbach, H., Bell, B., Berrisford, P., et al., 2020. The ERA5 Global Reanalysis. Quarterly Journal of the Royal Meteorological Society. 146(730), 1999–2049. DOI: https://doi.org/10.1002/qj.3803

[44] Soci, C., Hersbach, H., Simmons, A., et al., 2024. The ERA5 Global Reanalysis from 1940 to 2022. Quarterly Journal of the Royal Meteorological Society. 150(764), 4014–4048. DOI: https://doi.org/10.1002/qj.4803

[45] Sun, P., Xu, B., Wang, J., 2022. Long-Term Trend Analysis and Wave Energy Assessment Based on ERA5 Wave Reanalysis along the Chinese Coastline. Applied Energy. 324, 119709. DOI: https://doi.org/10.1016/j.apenergy.2022.119709

[46] General Bathymetric Chart of the Oceans (GEBCO), 2023. Gridded Bathymetry Data. Available from: https://www.gebco.net/data_and_products/gridded_bathymetry_data/ (cited 1 December 2025).

[47] U.S. Army Corps of Engineers (USACE), 2002. Coastal Engineering Manual (EM 1110-2-1100). U.S. Army Corps of Engineers: Washington, DC, USA.

[48] Zhai, R., Huang, C., Yang, W., et al., 2023. Applicability Evaluation of ERA5 Wind and Wave Reanalysis Data in the South China Sea. Journal of Oceanology and Limnology. 41, 495–517. DOI: https://doi.org/10.1007/s00343-022-2047-8

[49] Shi, H., Cao, X., Li, Q., et al., 2021. Evaluating the Accuracy of ERA5 Wave Reanalysis in the Water around China. Journal of Ocean University of China. 20, 1–9. DOI: https://doi.org/10.1007/s11802-021-4496-7

[50] Marine Department, 2022. Hydrographic Charts and Tide Tables for the Gulf of Thailand. Marine Department: Bangkok, Thailand.

[51] Department of Marine and Coastal Resources (DMCR), 2023. Thailand Coastal Erosion Status Report 2023. Department of Marine and Coastal Resources: Bangkok, Thailand. (in Thai)

[52] Electricity Generating Authority of Thailand (EGAT), 2023. Thailand Power Development Plan 2023–2037: System Load Forecast and Generation Expansion. Electricity Generating Authority of Thailand: Nonthaburi, Thailand.

[53] Benjamins, S., Williamson, B., Billing, S.-L., et al., 2024. Potential environmental impacts of floating solar photovoltaic systems. Renewable and Sustainable Energy Reviews. 199, 114463. DOI: https://doi.org/10.1016/j.rser.2024.114463

[54] Nysted, V.S., Lindholm, D., Selj, J., et al., 2024. Floating Photovoltaics: Modelled and Experimental Operating Temperatures and the Impact of Wind Speed and Direction. EPJ Photovoltaics. 15, 23. DOI: https://doi.org/10.1051/epjpv/2024020

[55] Forman, E., Peniwati, K., 1998. Aggregating Individual Judgments and Priorities with the Analytic Hierarchy Process. European Journal of Operational Research. 108(1), 165–169. DOI: https://doi.org/10.1016/S0377-2217(97)00244-0

[56] Mavraki, N., Bos, O.G., Vlaswinkel, B.M., et al., 2023. Fouling Community Composition on a Pilot Floating Solar-Energy Installation in the Coastal Dutch North Sea. Frontiers in Marine Science. 10, 1223766. DOI: https://doi.org/10.3389/fmars.2023.1223766

[57] Alcañiz, A., Monaco, N., Isabella, O., et al., 2024. Offshore Floating PV–DC and AC Yield Analysis Considering Wave Effects. Energy Conversion and Management. 300, 117897. DOI: https://doi.org/10.1016/j.enconman.2023.117897

[58] International Energy Agency Photovoltaic Power Systems Programme (IEA-PVPS), 2025. Floating Photovoltaic Power Plants: A Review of Energy Yield, Reliability, and Maintenance. IEA-PVPS: Paris, France.

[59] Micheli, L., Sepúlveda-Vélez, F.A., Talavera, D.L., 2024. Impact of variable economic conditions on the cost of energy and the economic viability of floating photovoltaics. Heliyon. 10(12), e32354. DOI: https://doi.org/10.1016/j.heliyon.2024.e32354

[60] Thailand Greenhouse Gas Management Organization (TGO), 2023. Thailand's Grid Emission Factor 2023. Thailand Greenhouse Gas Management Organization: Bangkok, Thailand.

[61] Opricovic, S., Tzeng, G.-H., 2004. Compromise Solution by MCDM Methods: A Comparative Analysis of VIKOR and TOPSIS. European Journal of Operational Research. 156(2), 445–455. DOI: https://doi.org/10.1016/S0377-2217(03)00020-1

[62] Solangi, Y.A., Shah, S.A.A., Zameer, H., 2019. Assessing the Solar PV Power Project Site Selection in Pakistan: Based on AHP-Fuzzy VIKOR Approach. Environmental Science and Pollution Research. 26(29), 30286–30302. DOI: https://doi.org/10.1007/s11356-019-06172-0

[63] Magkouris, A., Rusu, E., Rusu, L., et al., 2023. Float-

ing Solar Systems with Application to Nearshore Sites in the Greek Sea Region. Journal of Marine Science and Engineering. 11(4), 722. DOI: https://doi.org/10.3390/jmse11040722

[64] Huang, L., Elzaabalawy, H., Sarhaan, M., et al., 2025. Developing Reliable Floating Solar Systems on Seas: A Review. Ocean Engineering. 322, 120525. DOI: https://doi.org/10.1016/j.oceaneng.2025.120525

[65] Jin, R., Geng, B., Zhao, X., et al., 2025. An Overview for Offshore Floating Photovoltaic Structures and Their Fluid Dynamic Issues. Physics of Fluids. 37(6), 061301. DOI: https://doi.org/10.1063/5.0272574

[66] Xu, P., Zhang, Z., Li, S., et al., 2024. Numerical Investigation into the Dynamic Responses of Floating Photovoltaic Platform and Mooring line Structures under Freak Waves. Journal of Marine Science and Engineering. 12(1), 96. DOI: https://doi.org/10.3390/jmse12010096